

Customer Churn Prediction using Quotation Data

Master Thesis

Submitted on: May 2, 2022

at the University of Cologne

Name:	Abdurahman Maarouf
Address:	Schulstrasse 31
Postcode, Area:	53332, Bornheim
Country:	Germany
Matriculation number:	736481
Supervisor:	Prof. Dr. Dominik Wied

Contents

1	Introduction	1
2	Problem	2
2.1	Understanding the Problem	2
2.2	Idea	4
2.3	Literature Review	5
3	Methods	7
3.1	Data Preparation	8
3.2	Modelling Structure	16
3.3	Dimension Reduction	17
3.4	Handling Class Imbalance	20
3.5	Machine Learning Models	24
3.6	Model Evaluation Metrics	37
3.7	Explainability of the Models	39
4	Results	44
4.1	Exploratory Data Analysis	44
4.2	Modelling Baseline	48
4.3	Modelling Results	50
4.4	Comparison of GBT and EBM	61
5	Conclusion	66

1 Introduction

Predicting churners in order to retain customers has become one of the most important issues for companies in the area of Customer-Relationship-Management. With the exponential rise of data availability in the recent two decades, companies develop tools and methods to detect potential churners before they leave. More precisely, their goal is to estimate probabilities for a churn per customer in the next period of time. To tackle this issue, more and more advanced Machine-Learning-Algorithms are used guaranteeing solid accuracy in their out-of-sample predictions.

Fortunately for most of the companies, churn rates from one period to another are very small. However, in classification models predicting a rare event can become challenging. In this so called "Imbalanced Classes" issue certain arrangements to the underlying training data or the selected loss function need be made. Without these arrangements and with highly imbalanced classes, a poor algorithm simply never predicts the outcome of the minority class. In a dataset with 1000 customers containing 5 churners for example, this loss-minimizing algorithm would have an accuracy of 99.5%.

In order to avoid the high number of false-negative classifications there are many methods ranging from upsampling the minority class or downsampling the majority class to more advanced techniques like custom loss functions. In this work we present and compare the different methods while applying them to the underlying problem.

In this work we want to emphasize the importance of using quotation data for predicting customer churn. A company can track (potential) customer behavior on their distribution channels. Nowadays, in most cases the products or services are offered online on websites, which makes it easy to track website visitor data. In the context of dealing with customer churn this data can be matched to the customers already having a product or contract of this company. We show that first the number of visits of a current customer in the last period and second the average of the seen price during the visits have a high importance when predicting the probability of that customer leaving in the next period.

Another task of this work is to evaluate and interpret the importance and relationship of not only the quotation variables but also the other explanatory variables with the predicted outcome. In terms of explainability and interpretability, there is typically a trade-off during model selection. The trade-off

lies between the model complexity and the model interpretability. Gradient boosted trees (GBT) belong to the complex models which are famous for their comparatively high accuracy in almost all domains involving tabular data applications. Explaining and interpreting the resulting GBT by its model structure becomes almost infeasible.

However, in the course of this work and in many other areas understanding how explanatory variables interact with the outcome of the model becomes desirable. Knowing what the main drivers for high churn probabilities are can increase the scope of action the company has for retention strategies. The most transparent models in terms of interpretability are linear or logistic models. There the magnitude and sign of the corresponding coefficients (after being tested for significance) illustrate the changes of the outcome for a change in the specific explanatory variable. These models lack in terms of predictive performance when being compared to the complex ones, because they do not allow for non-linearities and interactions in the explanatory variables. Extensions, like general additive models (GAMs) [11] or GAMs allowing for pairwise interactions (GA²Ms) [18] incorporate non-linearities.

In this work we focus on comparing (1) the predictive performance and (2) interpretability of black-box and white-box models. For the black-box model we fit GBTs [8] as they outperform other models in most applications with tabular data. Partial dependency plots [7], Shapley values [19] and LIME [25] are novel approaches designed to make these black-box models interpretable. Additionally we present "Explainable Boosting Machines" (EBM) developed by Microsoft researchers Lou et al. [24] which are based on GA²Ms and are therefore interpretable in the form of their shape functions. EBMs aim to combine the high predictive performance of complex models on the one hand and the interpretability of general additive models on the other hand.

2 Problem

2.1 Understanding the Problem

For this work we use an applied problem of a big insurance company in Germany. Due to data protection the real data is not used. We however provide a sample data set, which resembles the real data in distribution, variables and statistical relationships. We focus on the product of automobile liability in-

surance, which is by law a mandatory service every car owner must hold in Germany.

Typically, car owners close a deal with an insurance company which can be terminated by the end of each year. In rare cases both sides agree on a contract with a due date during the year. If the contract does not get terminated, it is automatically extended for another year. Besides the option to terminate the contract at the due date there is also an option to terminate it earlier in a few special cases. These cases mainly involve the exceptional right of termination given to a customer. Here are the two most frequent reasons for this exceptional right, in which a churn can (but not must) occur before the contract due date:

Event A: Contractor is involved in an Accident.

Event N: Contractor buys a new Car.

The problem of predicting churn needs to be separated into the probability of a costumer leaving before his contract due date and churns happening at the due date. The reason is that the optimal modelling approach and explanatory variables have proven differences. One example is the premium adjustment send to the customers before their due date, which has a high contribution to the decision of the customers at the due date. Meanwhile, churns before the due date are dependent on the occurrence of the events A and N . In this work we focus on predicting churns occurring before the due date.

The purpose is to build a model which can be used at any time t of the year to predict the probability of a costumer leaving the company in the next period of time $(t, t + s]$ and not at his due date. It can be argued that in order to provide a model with maximized utility for production one would want to keep s small. For example a company would highly benefit from a model, which can predict the churn-probability of the next week. However we see that having a small s decreases the accuracy of our models, creating a trade-off situation between model accuracy and the benefits of a small s . With a smaller period the classes of the data become more imbalanced, creating a higher challenge of feeding the model enough information about churners. Furthermore, a small s decreases the scope of action for a company to retain potential customers leaving.

2.2 Idea

This work stands out in its novel approach of using quotation data for churn predictions. We are not aware of similar research in the literature utilizing that type of data. In the following we clarify what our understanding of quotation data is.

Through every distribution channel a company offers its product, (potential) customers leave behind a lot of useful data. These distribution channels can either be online websites or also offline agencies. In our insurance application (potential) customers must give specific information about themselves and their car they want to insure such that a price can be calculated. Every time a price is calculated all the information corresponding to that calculation is saved as a new row on the companies' database. From now on we define a price calculation as a request.

Main applications of quotation data involve price and new-business optimization, demand forecasting and conversion modelling. Another application however is to use this data in order to analyze the behavior of customers which already have an active contract. The main advantage is that (potential) customers having to enter their and the cars information. This entered information can be used to match an active customer with his/her requests.

In a prediction model information generated from quotation activity of time period $(t - m, t]$ can be used as explanatory variables. What type of quotation variables we generate is explained in chapter 3.1.

Hypothesis

The hypothesis of this work is that an active customer with high request activity is most likely looking for a new insurance contract. This would directly influence the churn probability. We test this hypothesis by: (1) Evaluating model predictions on unseen data with and without quotation data (2) Interpreting the models in terms of relationship between quotation variables and predicted outcome.

2.3 Literature Review

There is a wide range of literature covering supervised classification techniques and their usage for customer churn prediction. Verbeke et al. [32] provides an overview table on the literature dealing with churn modelling in static settings using cross-sections of data. It provides an extensive benchmark of classification methods and machine learning models applied to different data sets.

Some works have a different approach in modelling customer churn. Van den Poel et al. [31] for example models the time to churn using survival analysis techniques. This allows flexible estimations for the conditional probability of customer i churning in the next s periods of time, where the probability can be calculated for different values of s by the model structure itself. Given the fact that with survival analysis, conditioning on multiple time dependent variables is not possible or not well studied yet, we focus on modelling churn probabilities in the static setting.

The popularity of (deep) neural networks has risen enormously in the last two decades. Its promising accuracy in computer vision, natural language processing and sequential data in general are the reasons for its broad coverage in research. It has also found its way to modelling customer churn, as in [20], [29], [35], [38], [13] and [21]. All cited papers rely on the fact that customer data can be used as sequential data with time varying variables. Therefore, model architectures like convolutional neural networks (CNN) and long short-term memory networks (LSTM) come into play. We however focus on classification techniques which do not assume dependencies in the data points, given the data that we have available.

The different data preparation, preprocessing and variable engineering approaches for churn modelling are also extensively studied. [6] for example studies the data preparation approach for modelling churn probabilities in the telecommunication industry. They suggest that an appropriate selection and engineering of variables is essential to guarantee robust results and high accuracy. We apply their suggestion to some of our variables, which however differ due to the different setting.

Regarding preprocessing, Gattermann-Itschert et al. [10] underline the importance of multi-slicing. This technique essentially uses multiple time-slices T in the past to train the underlying models. They find out that this technique results in higher accuracy and robustness, which also holds true for our application.

As already stated, class imbalance naturally occurs in most churn prediction applications due to the fact that churners are less frequent than non-churners. This problematic increases in a contract setting, where there are only a few events which allow for an earlier termination than the due date. Weiss et al. [36] provides an overview on multiple techniques to handle class-imbalance. It especially highlights the effectiveness of sampling and cost-sensitive learning which prove to be the best techniques in our application as well.

Zhu et al. [41] offers a useful guideline of sampling methods in the context of churn prediction. It compares different sampling techniques in their effectiveness and multiple evaluation metrics. Burez et al. [3] extensively underlines the importance of using appropriate evaluation metrics in a churn prediction context. This not only increases the success of churn prediction models in practical settings. It also provides trustworthy metrics in order to make models more comparable.

It is important to note that in the applications of predictive analytics, two different evaluation approaches exist. Out-of-sample evaluation uses unseen samples from the same period(s) the model was trained on. Out-of-period evaluation tests the model on samples from a more recent period, which was not used for training. While out-of-sample evaluation is more dominant in the literature, Zahavi et al. [37] and Neslin et al. [23] emphasize the importance of evaluating the performance of the model on periods beyond the ones it is trained on.

Out-of-period evaluation is particularly important when there are time varying factors which influence the churn rate. Examples of such factors are demand, supply, competition, inflation and pricing. Especially in our use case with automobile liability insurance, products of competitors are close substitutes. So any change in the stated factors has high effects on customer behavior. This undermines the relevance of using multiple time slices for training and out-of-period evaluation.

A few research groups have focused on the choice of appropriate explanatory variables in the context of churn prediction. More specifically, there has been work done in the direction of using customer behavior to predict churn probabilities. Khodabandehlou et al. [15] applies multiple variables reflecting the behavior of customers in a grocery store setting. It also compares different models and highlights the importance of including such variables in production as they help ensuring high accuracy. These variables however focus on the buying and returning behavior under different discounts offered.

Calzada-Infante et al. [4] examines social-network behavior of customers in the telecommunication industry and their predictive power for churn probabilities. The researchers propose a novel tree-based modelling technique called similarity forests, which relies on social network analysis methods. Their work verifies that the behavior of customers, in their case social relationships, has significant predictive power. Zhang et al. [39] solely examines one class of behavioral data to predict telecommunication churn prediction, purposely excluding all other relevant variables. It focuses on variables generated with customer service data and also provides evidence for the importance of behavioral data. Moertini et al. [33] conducts research on supplier churn on e-commerce platforms while using quotation data. The hypothesis the researchers prove to be correct is that the frequency of supplier activities has high predictive power regarding their tendency to churn. They find out that the relationship in this B2C setting is negative, a low frequency of supplier activity goes along with a higher probability of a churn.

However, none of the above and to our best knowledge no other papers focus on using quotation data reflecting recent behavior of customers to predict churn probabilities. While [15], [4] and [39] all use customer-specific behavioral data, they all use different approaches of reflecting behavior. Also, their approach does not allow for monitoring individual recent changes in the behavior of customers and its impact on the churn probability. This turns out to be crucial for modelling churn using quotation data. In [33] the type of data used is the nearest to our, the researchers however apply it to supplier churn prediction. The novelty of this work is also reflected in the fact that while evaluating the models, we not only consider evaluation metrics on hold-out sets. We also use modern explainability approaches and compare their ability to represent relationships of explanatory variables with the target variable. With the lately rising necessity of interpretability we want to shed light on our modelling approaches to understand the driving forces which lead to high (or low) probabilities of churn.

3 Methods

In this section we present our methods and approaches utilized to build a churn prediction model. To fully capture the concepts we use in this work, we start

with the data preparation. Then we explain and compare methods to handle imbalanced classes. The next subsection introduces the theoretical and mathematical background behind the utilized machine learning models. Questions on how to properly evaluate these models with the appropriate metrics and how to make them interpretable are answered in the last two subsections.

3.1 Data Preparation

As in most machine learning applications data preparation is the most time-consuming part in this work. To have a clean and suited training dataset for modelling and a dataset for production is essential to guarantee accurate, robust predictions and interpretations. Therefore, we present the main issues in the raw data that are solved during data preparation.

The raw data comes from three main sources. The first source is a valid-time-state-table (VTST) containing all historic and present customer contracts information of the product automobile liability insurance. It contains valid-from and valid-to columns which makes it easy to extract information on the status, the car and the insurance holder at any point in time t . The second source table is also a VTST but contains historized accident data reported by an insurance holder. Finally, the quotation table is the third source, where simply the number of rows equals the total number of requests generated across all distribution channels.

The data preparation can be split up into 5 main steps, which are explained bellow and visualized in figure 1.

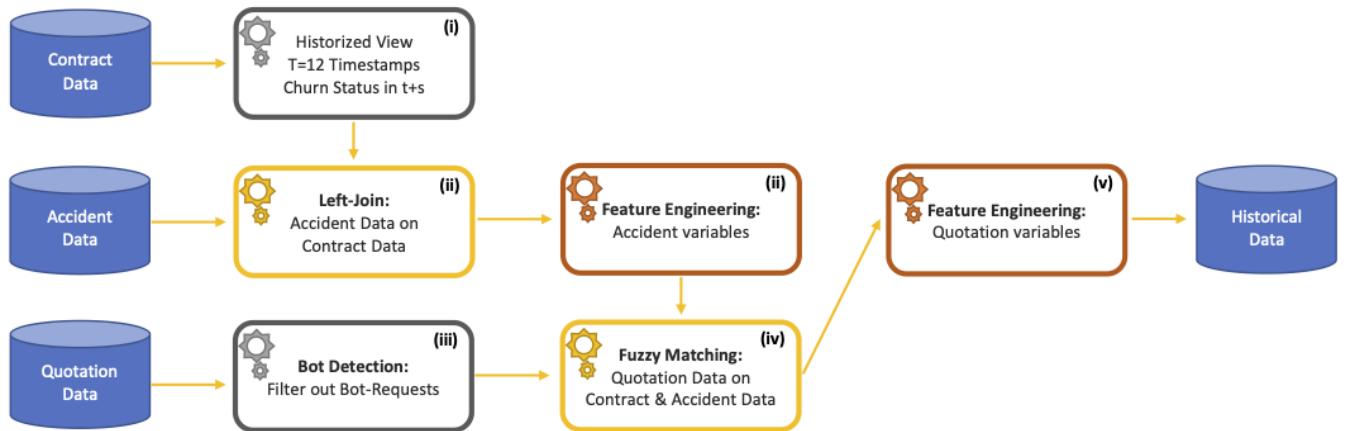


Figure 1: Vizualization of Data Preparation

(i) Creating the historized view of the Contracts

As already mentioned, the source table containing all contract information is a VTST. So, any desired point in time t in the past can be selected to collect all active contracts to that time. We use $T = 12$ points in time in the past, following the findings of Gattermann-Itschert et al. [10], to ensure a larger dataset and higher generalizability and robustness over time. That is why we generate 12 different tables in the first step, which are essentially views on the source table for the given points in time.

For each generated view-table (for each point in time t) and for each active contract we look for the status of that contract in $t + s$. This is done by joining the same table filtered for timestamp $t + s$ on the unique identifier column "contract_number". To ensure we only collect mid-contract-churns, we check if the termination date of that contract is unequal to the agreed upon termination date. The case where both dates are equal is excluded in our modelling question and therefore not seen as a churn.

The 12 points in time are selected carefully, in a sense that there is no overlapping between any time window $(t, t + s]$. So, following property must hold for any pair of time sets: $(p, p + s] \cap (q, q + s] = \emptyset$ for all $p \neq q$ and $p, q = 1, \dots, 12$. The final step for generating a historized view of the contracts is to create a union on all 12 subviews, creating a panel-dataset. The number of resulting rows after this operation equals the number of rows after all next steps. As a result of the union, we have already generated the framework of the prepared table. The only thing which is left is to generate more variables, especially accident and quotation variables.

(ii) Join accident data

In many modelling problems in the insurance context, it turns out that the driving behavior of the customer plays a big role in predicting the desired outcome. Especially in risk modelling, knowing how many times a customer was involved in an accident or how costly these accidents were, ensures good predictions.

Being involved in an accident is one of the events which give a customer the exceptional right of terminating the contract. Therefore, we also include historized accident data to generate explanatory accident variables. The VTST containing the historized accidents are recorded for each "contract_number",

which makes it easy to join the data to the table generated in (i).

We engineer two new variables based on the accident data. One is a simple count of accident the contract holder was involved in since the start of the contract ("n_accident"). The second one is the sum over the incurred costs corresponding to the accidents ("sum_accident_cost"). This quantifies the accidents and makes them comparable.

(iii) Bot Detection in Quotation Data

One big issue arises with the usage of quotation data. Not all requests in online distribution channels are generated by humans. The pricing information of a company is valuable for competitors' pricing strategy or other third-party institutions. As a result, many bots or crawlers are designed to automatically extract data from websites. The proportion of not-human requests can be very high and reaches up to 70% in one of the distribution channels.

As we do not want to consider bots and crawlers and falsely join them as requests from our active customers, we need to find a way to detect them. The first-best strategy would be to label a proportion of requests as $BOT = True$ or $BOT = False$ and then train a model to estimate $P(BOT = TRUE | X)$ for the remaining requests. This however is infeasible as there is no information on the true labeling for any request.

The second-best approach flags requests with unreasonably high number of same occurrences and is used in this work. Thus, it counts the number of requests with the same combination of certain quotation variables (1) over a day and (2) over the entire timeframe. These variables for flagging bots or crawlers should be as unique as possible in a sense that requests coming from the same source are only counted. For both (1) and (2) individually, a certain cutoff percentile of the combinations is specified. A request is then specified as a bot if the rank of its specific combination is larger than the cutoff.

The cutoff percentile is defined for every distribution channel individually (as some are more prone for bots than others). How to choose the correct cutoff is done through eyeballing the smoothness of distributions for suitable quotation variables. An example is the variable "time_of_day", where we have an expected distribution and can detect anomalies with our eye.

Figure illustrates the result of the bot detection algorithm and the distribution of "time_of_day" over the entire time since 2018 for one specific online distri-

bution channel. It is a screenshot of the dashboard which is used to monitor the performance of the algorithm. It was also used to finetune the cutoffs for every distribution channel and to choose the right combination of variables. The spikes between 2:30 am and 4:30 am clearly represent such an anomaly and are fully captured by our bot detection algorithm.

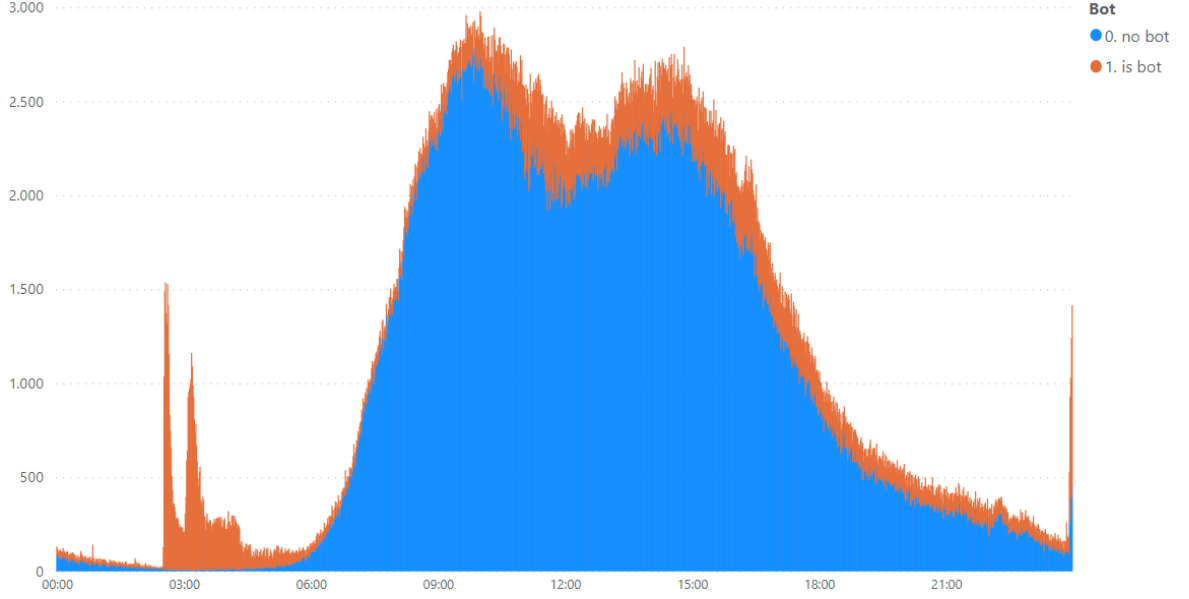


Figure 2: Bot Detection Results using "time_of_day" as an example

The advantage of this algorithm is that it also captures newly arriving bots by calculating percentiles per day. Also, it is able to treat the distribution channels individually. The algorithm parameters are easily adjustable and the performance is monitorable. It however still fails to capture certain types of bots which are programmed to enter a different combination of variables in each request. There however, it is nearly infeasible to detect them with any advanced method. In this work we estimate that these bots only make up a very small fraction of the requests and therefore we neglect them.

(iv) Matching quotation with contract data

Another issue with the quotation data is that there is no unique identifier column which can be used to correctly join it to the table generated in (i) and (ii). Additionally, columns like "name" or "birthdate" are not always correctly specified during their price request which makes the matching even more difficult.

If specified correctly in the quotation data, a combination of these variables could be used as key columns.

In order to address this $M \times N$ -Matching problem we need to come up with a fuzzy-matching algorithm. On one side we have a table which contains contracts at different timestamps, their status 2 months later and historic accident information. At the other side we have an ungrouped and unstructured table which simply lists all requests and their corresponding request information. The end result should be of the same structure as the base table created in (i) and (ii) but simply appended with the variables generated from quotation data. We can already expect that not all contracts have quotation activity m months before t . Also, not every request is associated with a contract holder. These two facts increase the uncertainty of matching but are necessary to check the scope and quality of matching.

The main idea behind our fuzzy-matching algorithm is to try to match both tables with a different set of signals iteratively. Each signal is a collection of variables which together serve as almost unique identifiers. One example for a signal is the combination of the variables: "hsn" (manufacturer key number), "tsn" (type key number), "plz" (postal code) and "birthdate".

As we join the quotation table on the contract table multiple times with different sets of signals we expect and first allow for duplicates of same "contract_id" \times "timestamp" combinations and/or requests. Therefore, the next important step in this section is the deduplication. We know that first the combination of "contract_id" \times "timestamp" and second request_id should be unique in the end table.

The first step of deduplication is to only include requests for each contract, which occurred in the corresponding request window $[t - m, t)$.

The matching algorithm is designed in a way that it implicitly allows to formulate preferences about the matching signals. So, to each signal a preference rank is associated. This is used for the second step of deduplication. To further eliminate duplicates, we only keep the most preferred match per "contract_id" \times "timestamp" combination on the one hand and per "request_id" on the other.

After the second deduplication step there might still be unwanted duplicates if for example the same requests are joined to different contracts with the same signal preference. To address this last issue, we pick the request-contract pair with the smallest time difference. This of course is not always the correct pair but ensures wrong duplicates. Additionally, there is no other information to

be exploited for correct matches. Unwanted duplicates occurring after deduplication steps 1 and 2 are however very rare (0.002%) and therefore can be neglected.

Like for the bot detection we generate a dashboard to monitor the quality of the matching algorithm. We have developed three checks which are automatically executed every time the data preparation is performed. We present them shortly in the following.

For all the checks we exploit the fact that every new-business contract, so a newly closed deal between customer and insurance, needs a corresponding request in the quotation data. Therefore, we use the same matching algorithm, but instead of joining the quotation data on our base contract table from (i) and (ii) we join it on a new-business table. With a perfect matching algorithm, we would expect a match rate of 100%. While monitoring our algorithm a match rate of 100% should however be regarded critically as it might be a result of too weak signals.

The first check is done by eyeballing the aggregated match-rate of the new-business-contracts over time. In the graph of figure 3 the x-axis represents the starting date of the new-business contracts and the y-axis the match rate to these contracts. The graph shows that the performance of the algorithm is stable and accurate as in the entire time window for over 90% of the contracts the corresponding request is found. The drop after November 2021 should not be misinterpreted as the plot was generated in November 2021.



Figure 3: Match Rate; Evaluation of Fuzzy Matching

To also ensure the correctness of the matches we monitor the quality by com-

paring the price determined in the new-business contract with the price of the matched request. Prices are not used in any matching signal for two reasons. One is the fact that after a converted request there may occur specific rebates or other changes to the price which lead to differences between contract price and request price. The second reason is to have an unbiased check of the matching-quality.

The resulting second check is generated with the visual in figure 4 where the percentage deviation between contract price and request price are binned into buckets for all new-business contracts. We expect some deviation around plus and minus 20% for given reasons. Abnormal differences over the 20% mark indicate a bad match.

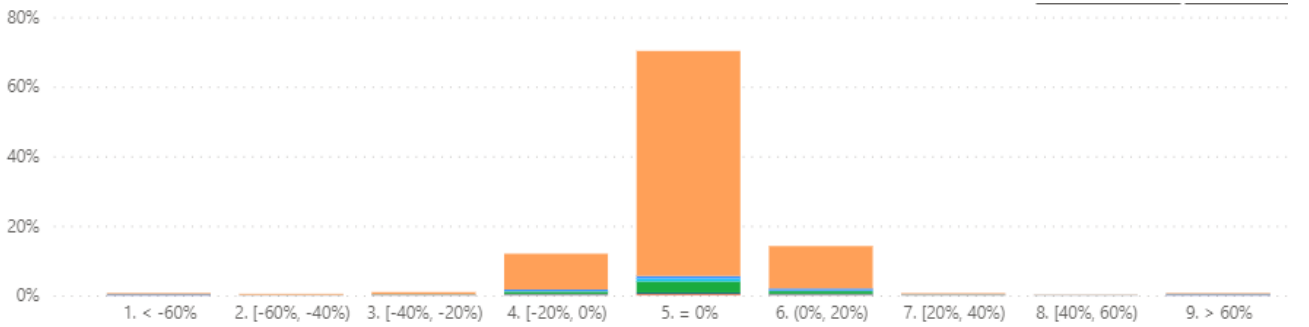


Figure 4: Match Quality; Evaluation of Fuzzy Matching

As we can see, after optimizing the matching signals and preferences bad matches occur in only a very small proportion. Additionally, we can safely say that a minimum of 70% of the contracts are correctly matched with its request as prices are exactly equal in these cases. Adding the expected deviation of contract and request price we are left with a good quality of matching. The third check also uses the new-business contracts as a test table for the performance of the algorithm. The idea behind this check is however to ensure that the current implementation is the best possible with the underlying data. We therefore model the match status (boolean) of the new-business contract as target variable and all underlying quotation and contract variables as explanatory variables. The model itself is a decision tree. The defining rule to decide whether the algorithm is using the most out of the given information is the resulting variable importance score. More specifically we use the score which assigns its overall contribution to loss reduction to each variable. So for each variable we calculate the decrease in node impurity weighted by the

probability of reaching that node.

Under full exploitation of the information at hand the decision tree should not be able to find a structure to model the match boolean. In result we should expect complete randomness in the structure of the tree and almost equal variable importance scores for all the variables. If there is any variable with abnormal high variable importance it is a sign for incomplete information usage for matching.

(v) Generating quotation variables

The last step of data preparation involves the feature engineering of quotation variables. The variables we generate can be summarized into four groups:

(1) $n_requests_m_{t-m,t}$: To each active contract we calculate the number of requests generated by the corresponding customer in the m months before the selected timestamp t . We allow for multiple values of m , more specifically $m \in \{1, 2, 3\}$, resulting in 3 different generated variables for this group.

(2) $diff_n_requests_m_{t-m,t}$: We also calculate the average monthly number of requests in the last m months subtracted by the average monthly number of requests in the last 12 months. The idea behind this group of variables is that it reflects if there is a difference in request behavior of the last m months to the normal behavior. So $diff_n_requests_m_{t-m,t}$ can be seen as a normalized version (using customer specific averages) of $n_requests_m_{t-m,t}$.

(3) $diff_avg_vjb_requests_m_{t-m,t}$: Here we use the average shown price of the requests and subtract it with the price the customer is paying according to his/her active contract. Again, we engineer 3 variables in this group, as $m \in \{1, 2, 3\}$.

(4) $diff_hsntsn_requests_m_{t-m,t}$: As customers have to state vehicle specific information during their price request, this information can be compared to the vehicle which is insured in the active contract. Thereby we concentrate on the "hsn" (manufacturer key number) and "tsn" (type key number). The combination of both the "hsn" and "tsn" is a unique identifier for the type of the car. Thus, for this group of variables we create a similarity score between

0 and 1. 0 reflects the case where none of the entered vehicles in the requests equals the "hsn"- "tsn"-combination in the contract and 1 is assigned to full similarity between requested car(s) and insured car. The resulting variables can be an indicator for the occurrence of event N , i.e. the customer thinking about changing his/her car.

Note that for each group we generate multiple variables with different values for m . Our purpose is to find the optimal request window m^* for each group using a dimension reduction technique called MRMR. This technique is presented in chapter 3.3 and is designed to optimally filter the variables when expecting correlation among them. This is highly reasonable for our quotation variables.

To summarize the data preparation, we present the challenges and methods used to generate a modelling-ready data-set. The steps needed to get to this end result are illustrated in figure 1. We are now ready to introduce modelling related methodologies used in this work.

3.2 Modelling Structure

To avoid overfitting and to ensure reliable and stable results we follow a strict modelling structure for our model approaches. Therefore we split the historical data set into a training (80%), validation (10%) and test set (10%). Thereby the splits are performed in a stratified manner, ensuring approximately the same proportion of churners in all subsets.

Every modelling approach involves two sets of hyperparameter (HP) tuning loops. We name the first loop the Structural-HP-Tuning-Loop (S-HPTL). This loop aims to identify the best set of all preprocessing HPs which involves the type of sampling, the type of dimension reduction and the type of objective loss function. The second loop nests in the S-HPTL and involves all model-specific HPs. We name this second loop the Model-HP-Tuning-Loop (M-HPTL). As it nests in S-HPTL, the entire loop of M-HPTL is executed in each iteration of S-HPTL.

Additionally, in each iteration of M-HPTL we fit the underlying model using a 3-fold cross-validation on the training set to ensure reliable training scores. The validation set is used for both GBT and EBM to evaluate the performance

of the model mid training. After having fitted all the candidates corresponding to the M-HPTL we pick the set of Model-HPs which yields the best evaluation scores. With this set of HPs, we fit the underlying model once more, but this time with the entire training set and no cross-validation. This model is used, tested on unseen data and presented as a candidate model for the corresponding set of Structural-HPs of the current iteration of S-HPTL. In a last step we manually compare all best candidates resulting from S-HPTL and pick the set of preprocessing HPs which yield the best evaluation scores. The figure 5 illustrates one iteration of the S-HPTL.

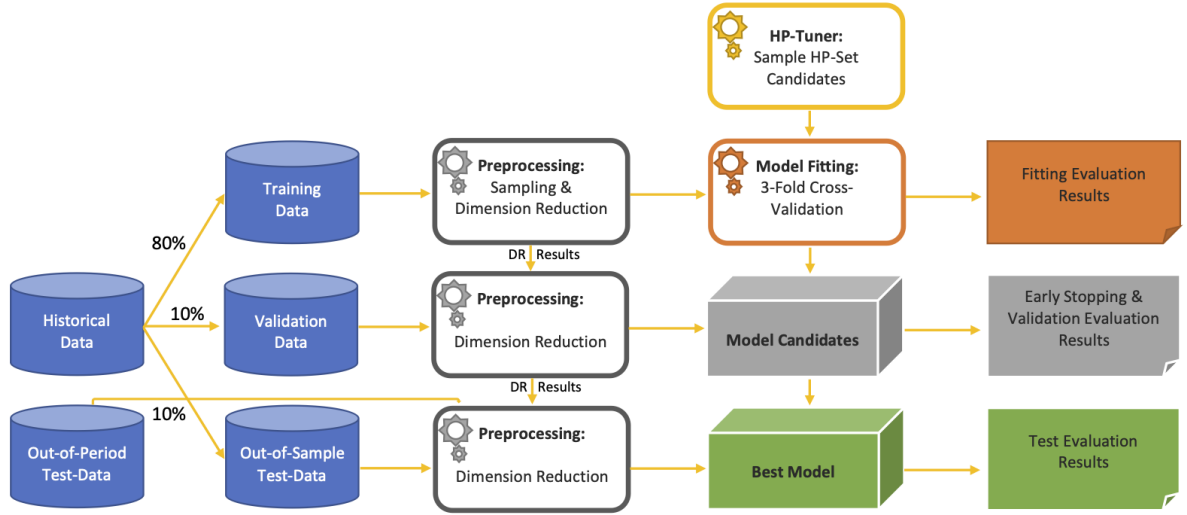


Figure 5: Modelling Structure; One Iteration of S-HPTL

This entire modelling approach is set up as it is to ensure reliable, robust and accurate results for the HPs, parameters, predictions and evaluation metrics. It additionally enables us to compare the different options of dimension reduction, sampling and the objective loss-functions presented in the following subchapters.

3.3 Dimension Reduction

A full collection of the explanatory variables in our data can be found in figure ???. As we most of the quotation variables we generate are highly correlated, preprocessing this data set is essential. The goal is to retain only the minimal

optimal subset of quotation variables. In many cases, due to multicollinearity in models with many variables, dimension reduction techniques can even improve the predictive performance of models.

In the current literature of machine learning there are many approaches for variable selection, ranging from manual selection to fully automated selection procedures. We use the "Maximum Relevance Minimum Redundancy" (MRMR) - approach designed by Uber's machine-learning researchers Zhao et al. [40]. The authors focus on designing an algorithm which detects the best subset of instead of the subset of best variables. The latter is often used in applications of machine learning, where a model is trained and the selection is performed a posteriori based on certain importance scores for that model. This however does not eliminate redundant variables, which do not improve the model performance in reality due to being already represented in correlated other inputs.

Using the best subset also helps us to identify the optimal length of the request window m per quotation variable group. As we want to examine the impact of quotation data for predicting customer churn, we include multiple number-of-request variables with different values for m in our unfiltered selection of variables F . These are obviously expected to be highly correlated, which additionally delivers a possibility to monitor the effectiveness of the MRMR.

MRMR works iteratively, so at each iteration a new best variable is identified and added to the list of selected variables. Once a variable is selected it cannot ever be unselected in the next iterations. One drawback of this approach is that the number of iterations and therefore the number of selected variables has to be predefined. We extend it however in a way that we iterate through the entire variable set F and cache the resulting sets and scores of each iteration. So, the resulting iterative process starts with an empty selected S and full unselected U set and ends with a full S and an empty U . This lets us define the optimal number of iterations retroactively.

The algorithm MRMR got his name from the fact, that at each iteration j a new variable is selected into S that has the maximum relevance with respect to the target variable scaled by the redundancy with respect to the variables that are already in S . Therefore, at each iteration and for each of the remaining variables in U the following score is computed:

$$score_i(variable_{i \in U}) = \frac{rel(variable_{i \in U}, C)}{red(variable_{i \in U}, variables \in S)} \quad (1)$$

The sets U and S get updated each iteration by transferring the variable with the highest score from U to S . In their paper, Zhao et al. present multiple metrics for both relevance and redundancy. We focus on one approach which yields the best result in their paper.

At each iteration the relevance of the remaining variables in U must be computed with a new model utilizing only these remaining variables. We use gradient boosted trees and its package "lightgbm" (LGBM) in python in each iteration to score the new relevance of each remaining variable. LGBM has a build in method for calculating variable importance which is used in this MRMR-setting to represent relevance of a variable. There, variable importance is computed as the number of times that specific variable is selected for a split. How gradient boosted trees work is explained in chapter 3.5.

For redundancy an average over certain standardized metrics for the relationship between the to be evaluated variable and the variables already in S needs to be computed. These metrics depend on the scales of measurement for the variables. Zhao et al. only cover the case of continuous variables and their relationship. We extend the redundancy score to categorical and binary variables. Thereby we pay attention to the fact, that the scores need to stay comparable for the different scales. Therefore, the chosen metrics (see [14]) are all standardized to values between 0 and 1, where 0 indicates no and 1 the strongest possible relationship. The different scale pairs and their relationship metrics can be summarized by table 1 (Cramer's-V-Correlation: C.-V-Correlation, Point-Biserial-Correlation: P.-B.-Correlation, Bravais-Pearson-Correlation: B.-P.-Correlation).

	nominal	binary	continuous
nominal	C.-V-Correlation		
binary	C.-V-Correlation	C.-V-Correlation	
continuous	Eta-Correlation	P.-B.-Correlation	B.-P.-Correlation

Table 1: Relationship Metric based on Scale

Redundancy is then calculated by the mean of the relationship scores as follows:

$$red(variable_{i \in U}, variables \in S) = \frac{1}{n(S)} \sum_{s=1}^{n(S)} relationship(i, s) \quad (2)$$

The slightly modified MRMR-approach we use can therefore be illustrated by this simplified pseudo-code:

Algorithm 1 MRMR-Algorithm

```

corrmatrix  $\leftarrow$  corr(X)
S  $\leftarrow$  []
U  $\leftarrow$  [X.columns]
cachedict  $\leftarrow$  {}
for j in range len(X.columns) do
    relvector  $\leftarrow$  LGBMscorer(U)
    redvector  $\leftarrow$  mean(corrmatrix [U] [S])
    scorevector  $\leftarrow$  relvector / redvector
    bestfeat  $\leftarrow$  max(scorevector).name
    bestscore  $\leftarrow$  max(scorevector)
    S.append(bestfeat)
    U.drop(bestfeat)
    cachedict.append(j, bestfeat, bestscore)
end for

```

As the type of dimension reduction is part of the S-HPTL, we use two different sets of explanatory variables as the sets of HPs. One set uses the best set of quotation variables as a result of MRMR. The other set excludes all quotation variables in order to indicate and evaluate the predictive power of quotation data.

3.4 Handling Class Imbalance

Studying the rarity of an event in the context of machine learning has become an important challenge in the recent two decades. Rare events, such as a customer churning in the next period, are much harder to identify and

learn for most of the models. HaiYing Wang et al. [34] study the convergence rate and distributional properties of a Maximum-Likelihood estimator for the parameters of a logistic regression while predicting rare events. Their finding is that the convergence rate of the MLE is equal to the inverse of the number of samples in the minority class rather than the overall size of the training data set. So, the accuracy of the estimates for the parameters is limited to the available information on the minority class, even if the size of the dataset is massive.

Some methods have been developed to decrease the problematic of imbalanced classes. In this chapter we present different methods which can be applied to the training set, before feeding it to the model. Also, we present different objective loss functions which also aim in solving the problematic. To handle and evaluate the outcomes of rare events prediction, appropriate models and model evaluation metrics must be chosen. This is discussed in the next two subsections however.

(i) Downsampling

The first basic sampling method is named downsampling. It randomly eliminates samples from the majority class in order to artificially decrease the imbalance between the two classes. The downside of this approach is that it possibly eliminates useful samples for the model to maintain a high accuracy in predicting the majority class [36]. HaiYing Wang et al. also study the convergence rate and distributional properties when applying downsampling. According to their findings the asymptotic distribution of the resulting parameters may be identical to the MLE's using the full data set. Under this condition there is no loss in terms of efficiency (minimum possible variance of an unbiased estimator divided by its actual variance).

(ii) Upsampling

The second basic sampling method is the upsampling approach. This method simply duplicates samples from the minority class to reach a higher balance. While duplicating samples though, the chances of overfitting to these duplicates becomes a more probable threat. Also, no new data is being generated in order to let the model learn more valuable variables about the minority

class [36]. Additionally, the computational performance of this approach can get rather poor, especially with large datasets and highly imbalanced classes. While evaluating the asymptotics of the MLE's with upsampling, HaiYing Wang et al. find out that it also decreases the efficiency. A probable higher asymptotic variance of the estimators is the reason for that.

(iii) SMOTE

The more advanced SMOTE approach (Synthetic Minority Oversampling Technique) [5] also creates more artificial samples of the minority class. Instead of simply duplicating some rows SMOTE creates new nearest neighbors in terms of variable values for the minority class samples. While constructing the variable values of the new sample ($N + 1$) as a new nearest neighbor for sample i one has to differentiate between continuous and nominal variables. The k -nearest neighbors for the minority class are typically constructed with the Euclidean Distance for continuous variables and the Value Distance Metric for nominal variables. The structure of one new-sample-creation for both types of data is presented in the next two paragraphs.

A Continuous variables:

- 1) Construct difference between corresponding variable value of sample i and one of its k nearest neighbors.
- 2) Multiply this difference with a random value drawn from a uniform distribution between 0 and 1.
- 3) Construct the variable value of the new sample by adding the multiplied difference to the variable value of sample i .

B Nominal variables:

- 1) Choose the variable value which is the majority vote between the variable value i and its k nearest neighbors.
- 2) Assign this value to the corresponding variable of the new sample.

With this approach it is ensured that the model learns more about the neighborhood regions of the minority class. It decreases the probability, that the model overfits to the duplicates created in upsampling. The drawback of this approach however is that the computational time is even higher than with

simple upsampling. Also, the new samples do not reflect real information and might therefore also lead to out-of-sample accuracy losses. The literature agrees on SMOTE's effectiveness is application dependent [36].

(iv) Cost-Sensitive Classifiers

One disadvantage of the up-to-now presented sampling methods is the need to change the data distribution. A different starting point is to alter the objective loss function which is minimized during the model fitting. Thereby the data size and the distribution stay the same. In the modified cost function we want to penalize false-negative classifications with a higher weight. Reason behind this is to ensure that the event of interest, represented by the minority class, is predicted correctly [30].

The challenge of this approach is to find the appropriate penalty parameters. It is hard to measure the cost of misclassifying an insurance-customer regarding churn-probabilities. The fact that these costs can come from multiple sources which are not easily definable is one part of the reasoning. We focus on two types of custom loss functions.

One conventional method is to assign simple parameter weights α and $1 - \alpha$ to the loss function. By default one might use the inverse of the class frequency as the associated weights. These parameters however can also be optimized during the structural HP-tuning loop. We call this method the "Simple Weighted Loss Function". The derivation is part of the next subchapter.

The second approach is called "Focal Loss Function" and was originally designed by FAIR (Facebook Artificial Intelligence Research) for an object detection purpose [16]. As it also aims to penalize false-negative classifications it is widely used for predicting rare events. Again, the exact structure of the modified loss-function is shown in the next subchapter and the parameters are tuned with the S-HPTL.

To conclude we present 3 sampling methods and two cost-sensitive loss functions. For our S-HPTL, we allow for a combination of both sampling and cost-sensitive learning at the same time, as they do not exclude each other.

3.5 Machine Learning Models

In this section we present and explain mathematical and statistical theoretics behind the machine learning approaches used to model churn in this work. As already stated, the two modelling approaches in this work are gradient boosted trees (GBT) and explainable boosting machines (EBM). GBT are selected due to its known predictive accuracy on tabular data. We compare it to EBM, which essentially aims to provide an explainable model structure.

In order to provide the mathematical and statistical intuition behind GBT and EBM, less complex models have to be explained first as they build upon them. That is why we start with logistic regression and classification trees and work our way up to the more complex models.

(i) Logistic Regression

The logistic regression is used as a benchmark model for all classification problems. It has high advantages in terms of computational complexity and interpretability but fails in capturing complex relationships and interactions. As it has the lowest accuracy of all classifiers it is mostly used as a baseline model in order to evaluate the advantages of additional complexity in the models, as in GBT and EBM. We however use a different baseline in our modelling approach and therefore only introduce it as the logic is needed for the more complex models.

Logistic regression applies a sigmoid function to the linear regression model in order to get output values (probabilities) between 0 and 1 as in a Bernoulli distribution. We use the following conventional notation throughout this work:

$$\hat{C}_{\{t+s\}} = P(C_{\{t+s\}} = 1 \mid X_{\{t\}}) = f(g(X_{\{t\}})) = \frac{e^{g(X_{\{t\}})}}{1 + e^{g(X_{\{t\}})}} \quad (3)$$

Note that from now on we use a vectorized notation. So $\hat{C}_{\{t+s\}}$ represents a vector of probabilities $(\hat{C}_{1,\{t+s\}} \hat{C}_{2,\{t+s\}} \dots \hat{C}_{N,\{t+s\}})$. The i 'th element ($i = 1, \dots, N$) corresponds to the probability of contract i churning in time $t + s$. This probability vector is constructed by a model conditional on a variable matrix X at time t . Again, each row of X represents a different contract and column j corresponds to variable j ($j = 1, \dots, M$).

Therefore $f(\cdot)$ is the sigmoid function used on function $g(\cdot)$, where in logistic regression $g(\cdot)$ is a linear model. For GBM and EBM this function is allowed to be more complex.

$$g(X_{\{t\}}) = \beta X_{\{t\}} + \epsilon_{\{t\}} \quad (4)$$

As the classification models output probabilities between 0 and 1 for a churn, a cutoff τ is needed in order to create assignments to each class. The rule of thumb is to set $\tau = 0.5$, such that probabilities larger than 0.5 are predicted as churns and the rest as non-churns. We see that the optimal τ is application dependent and relies on the type of sampling and loss function which is tried to be minimized. Typically, a high τ ensures that a high percentage of positive classified samples are in fact positive. A lower τ however ensures that a higher number of churners are detected (but with lower precision).

$$\hat{C}_{\{t+s\}}^{class} = \begin{cases} 1, & \hat{C}_{\{t+s\}} \geq \tau \\ 0, & \hat{C}_{\{t+s\}} < \tau \end{cases} \quad (5)$$

We apply Maximum Likelihood to estimate the vector of parameters β of the model. It maximizes the joint probability that the status of the contracts is drawn from the Bernoulli distribution stated in equation (3). For the final model in production, when estimating probabilities for a churn in the next period, t is of course equal across all contracts in X . But when it comes to training the model, as already stated, we use multiple timestamps of the historized data.

For the training part of this work, we therefore leave out the index t in order to avoid a misleading notation. $N^{train,k}$ corresponds to the number of samples in the k -th ($k = 1, 2, 3$) fold of the training data. As the model is retrained on the entire training set after cross-validation, $N^{train,full}$ samples are used in the equations below. We will generalize the notation with N^{train} which corresponds to $N^{train,k}$ during cross-validation and to $N^{train,full}$ during refitting. Still, the status of contract i is determined after s units of time for all contracts. The likelihood function to be maximized during training is described as follows:

$$\mathcal{L}(C; X, \beta) = \prod_{i=1}^{N^{train}} P(C_i = 1 | X_i)^{I(C_i=1)} \left(1 - P(C_i = 1 | X_i)\right)^{1-I(C_i=1)} \quad (6)$$

To describe this term as a loss function it is characterized by the negative logarithm of equation (6), which can be minimized with respect to β using Gradient Descent, Newton Raphson or other optimization methods.

1: Log Loss Function

$$\begin{aligned} l(C; X, \beta) &= - \sum_{i=1}^{N^{train}} C_i \log(P(C_i = 1 | X_i)) + (1 - C_i) \log(1 - P(C_i = 1 | X_i)) \\ &= - \sum_{i=1}^{N^{train}} C_i \log(\hat{C}_i) + (1 - C_i) \log(1 - \hat{C}_i) \end{aligned} \quad (7)$$

In applications with high dimensional data, it makes sense to add a penalty term to the loss function to avoid overfitting during training. While minimizing the loss function, this additional penalty term either shrinks some parameters of β towards zero (L2 regularization) or sets some to exact 0 (L1 regularization). However, we can also reduce the dimension of variables prior to fitting the model, as already explained with the MRMR-approach.

As already mentioned in chapter 3.4, one technique to handle imbalanced classes is to use cost-sensitive loss functions. We can implement this by setting additional penalty weights to our loss function. The resulting objective "Simple Weighted Loss Function" is described as:

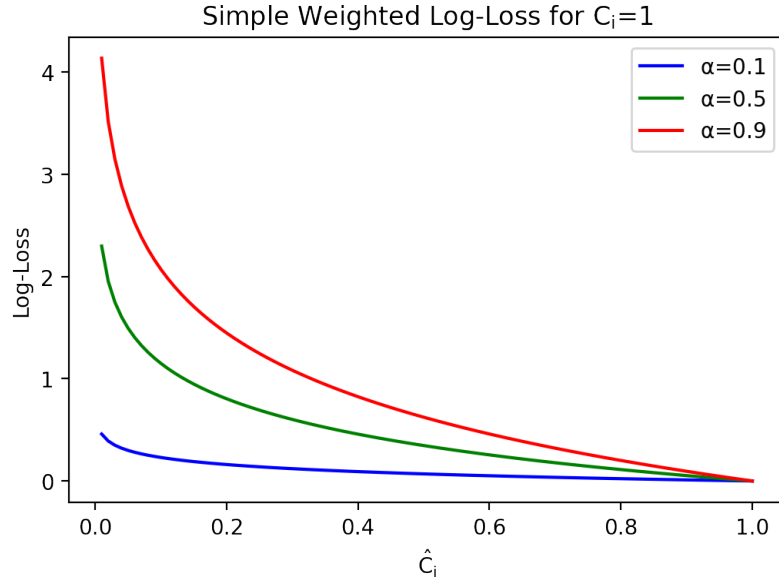
2: Simple Weighted Loss Function

$$l(C, \hat{C}) = - \sum_{i=1}^{N^{train}} \alpha C_i \log(\hat{C}_i) + (1 - \alpha)(1 - C_i) \log(1 - \hat{C}_i) \quad (8)$$

The additional parameter of α is a hyperparameters which can be tuned during S-HPTL. Following Gattermann Itschert et al. [10] approach, α can also be set by default to the inverse of the relative class frequency of the majority

class in the training data.

To provide further intuition behind the idea of using a weighted loss function we look at the individual loss for different values of α . For $\alpha > 0.5$ we reach the desired state of penalizing false-negative classifications more than false-positive ones. To see why this is the case it is best to look at the single log-loss for a positive sample. Positive samples in equation (8) can be seen as the insertion of $C_i = 1$ which simplifies the individual loss to $-\alpha \log(\hat{C}_i)$. For higher α , the loss gets higher for every \hat{C}_i . This example is visualized by the following plot:



This can be done analogously for negative samples. The individual loss for $C_i = 0$ simplifies to $-(1 - \alpha) \log(1 - \hat{C}_i)$. We therefore see that for $\alpha > 0.5$ the relative penalty for false-negative classifications is higher than for false-positives.

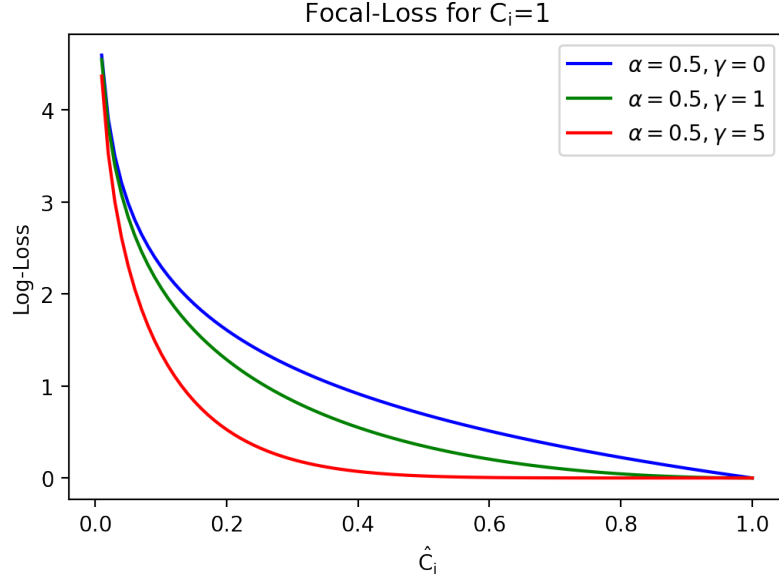
Going one step further and introducing one more adjustable parameter to the objective function we arrive at the "Focal Loss Function". It is structured as in equation (9).

Again, α and γ are hyperparameters, which are tuned during S-HPTL. Note that for $\gamma = 0$ (9) becomes a "Simple Weighted Loss Function". So the same intuition for varying weights α can be applied here. Also note that for $\gamma = 0$ and $\alpha = 0.5$ we are left with the original log-loss function derived in equation (7) multiplied by 0.5.

3: Focal Loss Function

$$l(C, \hat{C}) = - \sum_{i=1}^{N^{train}} \alpha(1 - \hat{C}_i)^\gamma C_i \log(\hat{C}_i) + (1 - \alpha) \hat{C}_i^\gamma (1 - C_i) \log(1 - \hat{C}_i) \quad (9)$$

To understand how γ can be used to improve modelling, we again look at the single loss for a positive sample $C_i = 1$. As γ affects the loss for positive and negative classifications analogously, the same logic can be applied for $C_i = 0$. Thereby we again plot the loss for different values for γ and \hat{C}_i and set $\alpha = 0.5$.



As illustrated a positive γ skews the function in a way that small to medium deviations of \hat{C}_i from the true C_i are not penalized as much as in the normal log-loss function. Strong deviations however are penalized almost as much as in the normal function. This introduces the effect of a higher relative loss for "bad" false classifications.

Both equation (8) and (9) aim to tackle the issue of having highly imbalanced classes. We use and compare both with different parameters in the S-HPTL and select the one which performs best on unseen data.

(ii) Tree-based Classifier

A Single Classification Tree:

Classification trees have a different approach on building a prediction model for $\hat{C}_{t+s} = P(C_{t+s} = 1 \mid X_t)$. Unlike linear or logistic regression, they allow for non-linearities and interactions. Classification trees search for the optimal sequential binary sample splits in order to minimize an inner objective loss function. So at each node of the tree the optimal variable j and its optimal split point r need to be found. The search at each node can be formalized as follows:

$$\begin{aligned} \{j, r\} \in \arg \min_{j, r} \quad & \sum_{i: X_i \in S_1(j, r)} L(C_i; X_i, \hat{p}_k) + \sum_{i: X_i \in S_2(j, r)} L(C_i; X_i, \hat{p}_k) \\ \text{with: } & S_1(j, r) = \{X \mid X^{(j)} \geq r\}, S_2(j, r) = \{X \mid X^{(j)} < r\} \end{aligned} \quad (10)$$

The loss function for region S_k is calculated using the resulting region prediction \hat{p}_k . This value is applied to all observations which are assigned to it after the splits $i : X_i \in S_k$. In a classification setting the prediction simplifies to the shares of churns in S_k . The typical loss functions are based on evaluating the purity of the resulting regions. In the ideal case, one would like to find the splits in X which always correctly assign contracts of the two classes into two different regions. In this case, \hat{p}_k would always be either 1 or 0. In order to approach this case one either uses the Gini-index or the Cross-entropy for region S_k :

$$\begin{aligned} \text{Gini-index:} \quad & 2\hat{p}_k(1 - \hat{p}_k) \\ \text{Cross-entropy:} \quad & -\hat{p}_k \log(\hat{p}_k) - (1 - \hat{p}_k) \log(1 - \hat{p}_k) \end{aligned}$$

The splits at each node are performed until certain criteria for the loss functions or other hyperparameters are met. Hyperparameters of a single tree are summarized in table 2. To get the prediction \hat{C}_i , one assigns \hat{p}_k as the region prediction of the corresponding end node of observation i to that value.

B Boosted Trees for Classification:

In most applications the predictions of a single classification tree have high variance due to overfitting to the training data. The accuracy in the prediction on unseen data is therefore rather poor compared to the accuracy during training. Random forests [2] are designed to reduce the variance, by averaging over predictions of multiple independent trees. This phenomenon is called "Wisdom of the Crowds". It is underlined by the fact that the average of multiple estimators for the same parameter has the same bias but a smaller variance (how much depends on the number of estimators) than a single estimator.

The current literature however agrees on the fact that gradient boosted tree algorithms outperform random forests, and therefore also a single tree. Therefore we focus on the core methodology and hyperparameters of boosted trees in the following.

The idea of boosted trees for classification is to have a sequence of dependent base learners (trees), which improve in terms of accuracy where it is most needed. Thereby, the base learners $\hat{g}_b(X)$ ($b = 1, \dots, B$) are constructed in a shallow shape, avoiding an overfitted single learner. Additionally the trees $\hat{g}_b(X)$ are now regression trees, which output values in $(-\infty, \infty)$. So, for the optimal split at the nodes of each tree the squared error reduction of the log-odds are now being compared. To get a probability in $[0, 1]$ we again have to apply the sigmoid function $f(\cdot)$. The resulting loss of each tree is then fitted by the preceding trees. So the procedure can be summarized by this pseudo code:

Algorithm 2 GBT-Algorithm

```
 $\hat{G}(X) \leftarrow 0$   
 $L \leftarrow \sum_{i=1}^{N^{train}} l(C_i, f(\hat{G}(X_i)))$   
for  $b$  in range(1, B) do  
    Fit tree  $\hat{g}_b(X)$  which minimizes  $L = \sum_{i=1}^{N^{train}} l(C_i, f(\hat{G}(X_i) + \hat{g}_b(X_i)))$   
     $\hat{G}(X) \leftarrow \hat{G}(X) + \lambda \hat{g}_b(X)$   
end for  
 $\hat{C} = \hat{f}(\hat{G}(X)) = f(\sum_{b=1}^B \lambda \hat{g}_b(X))$ 
```

The hyperparameter λ is called learning rate and set to a small number to learn slowly and to avoid overfitting. Also notice, that the loss function defined here is the objective loss function used for gradient boosting. It is different than the inner objective function used for constructing a single tree. We try both custom loss functions for GBT derived in equations (8) and (9) and perform hyperparameter tuning to get the best set of hyperparameters belonging to these loss functions.

To apply these custom-loss functions we need to derive the gradient as well as the hessian of this function. Herewith the `lightgbm`-package [8] aims to reduce computation time as it takes the second order taylor expansion to compute the optimal loss minimizing $\hat{f}_b(X)$ in each iteration $b = 1, \dots, B$. Gradient and hessian are calculated in the appendix.

The main time cost of GBT is learning the single trees, and the most time-consuming part in trees is to find the best split-points. Therefore we make use of an approach of the `lightgbm`-package which aims to tackle this issue. The so-called histogram-based approach is designed to bin the variables. This creates high efficiency gains while searching for the optimal splits, especially for continuous variables.

Another important aspect to note about `lightgbm`'s implementation of boosted trees is the fact that the base trees grow leaf-wise instead of depth-wise. As proposed by Friedman et al., the idea is to extend nodes in first-best order. Thereby, the best node is the one which maximally reduces the sum of the tree loss function in the resulting regions. This enables the possibility that a first-best split is found at a node in level $r + 1$ even though in level r only one of two nodes are split.

If we let the trees grow without tree structure restrictions to full trees, both the leaf-wise and depth-wise approach result in the same trees. As all gradient boosters rely on shallow trees, the combination of hyperparameters such as the maximum number of leaves, the minimum loss reduction required for a further split the first-best split approach results in a better shallow tree structure.

There are a lot of hyperparameters which allow to tune the model structure inside M-HPTL. They can be split into the hyperparameters for single tree structure and hyperparameters for the learning process. In table 2 is an overview of the hyperparameters we focus on and the corresponding values we use for grid search in M-HPTL.

	Hyperparameter	Grid Search Values
Boosting	Boosting learning rate λ	Shrinking learning rate
	Maximum Number of boosted Trees B	1000
	L1 regularization term on weights	$\sim [0, 1, 5, 10, 100]$
	L2 regularization term on weights	$\sim [0, 1, 5, 10, 100]$
Single Tree	Maximum number of tree leaves	$\sim U(6, 50)$
	Minimum loss reduction for split	0
	Minimum number of samples in new region	$\sim U(60, 500)$
	Subsample ratio of columns for tree	$\sim U(0.4, 1)$
	Subsample ratio of data for tree	$\sim U(0.4, 1)$

Table 2: Hyperparameter sets for M-HPTL - GBT

We make use of an early stopping criterium evaluated on the validation set. It terminates boosting when the loss function does not improve for 30 rounds. So, in each iteration and for each model-HP of M-HPTL we randomly sample from the corresponding distribution/set from table 2. To ensure generalizable results the current set of HPs in one iteration is evaluated by using cross-validation on the training data. For GBT we sample 100 times from these sets. Multiplying this with the 3-fold fitting, we are left with 300 fits in total resulting from the M-HPTL. The set of model-HPs which yields the best results in terms of evaluation metrics is refitted and selected as a model candidate for the current S-HPTL iteration.

Table 3 summarizes the sets of HPs used for the S-HPTL for GBT. "N" as a hyperparameter for sampling means that no sampling is performed, and the length of the training data remains the same. "d" (or "u") downsamples (or upsamples) the data such that both classes have the same number of samples. "dX" (or "uY") samples in a way that the number of samples in the majority (or minority) class is multiplied by X (or Y).

The normal log-loss function is minimized with the combination of α being "N" and γ being "N". For α having assigned a value and γ being "N" we optimize the "Simple Weighted Loss Function" defined in equation (8). If both parameters have a value, the "Focal Loss Function" from equation (9) is minimized. Additionally, in each iteration of S-HPTL, we run the M-HPTL with two dif-

ferent sets of variables. This is denoted by the row "Variables". More precisely, in each iteration of S-HPTL the best set of quotation variables is determined with MRMR. This is repeated every iteration since with different sampling methods, a different set of variables might be optimal. To determine the predictive power of quotation data, we once fit the current M-HPTL with and without quotation variables.

	Set
Sampling	[N, d, d0.1, d0.5, u, u10, u50, sm]
Custom Loss	α : [N, 0.6, 0.7, 0.8], γ : [N, 0.2, 0.5, 1, 2, 5]
Variables	[with_quot, no_quot]

Table 3: Hyperparameter sets for S-HPTL - GBT

For the S-HPTL we try out each possible combination of the values in the sets for sampling, α , γ and variables. These total $8 \times 4 \times 6 \times 2 = 384$ iterations for the structural loop. Adding to that the fact that in each iteration 300 models are fitted inside the M-HPTL, we end up with 115,200 models in total. This of course results in a computational complex task but ensures the needed comparability and optimal (hyper)parameters.

(iii) Explainable Boosting Classifiers

Explainable boosting machines (EBM) were developed by researchers at Microsoft [24] and aim to have high accuracy as most complex models, while maintaining an easy interpretable approach. It is maintained by the functional form which is similar to the standard GAM-Model, developed originally in 1987 by Hastie et al. [11]:

$$g(X) = \beta_0 + \sum_{j=1}^M k_j(X^{(j)}) + \epsilon \quad (11)$$

Thereby M is the number of variables and $k_j(\cdot)$ is the so called shape function for variable j . In standard GAM-models $k_j(\cdot)$ is approximated by scatterplot

smoothers. In EBM the approximation for $k_j(\cdot)$ is allowed to be calculated by a complex modern learner such as a decision tree or a random forest.

As the name of the method already reveals, gradient boosting is applied to improve the preceding trees in direction of the gradient of the loss function. The main difference to the standard gradient boosting classifier is that no longer one tree fits all variables $\hat{g}_b(X) = \hat{g}_b(X^{(1)}, \dots, X^{(M)})$ in each iteration $b = 1, \dots, B$. Instead in each iteration, the algorithm cycles through all variables to improve the single shape functions $k_j(\cdot)$, where it is most needed. By cycling through the variables one at a time and maintaining a low learning rate the variable order does not matter and the potential problem of multicollinearity is reduced.

Unfortunately, there is still a huge gap between standard GAM-models and full complexity models in terms of predictive accuracy, even if we allow for non-linearities in $k_j(\cdot)$. Full complexity models, such as gradient boosted trees and deep neural nets, have the advantage of allowing for an arbitrary number of interactions between variables. To allow for pairwise interactions, EBM's make use of the idea of GA²M-models developed by Lou et al. [18]. The resulting shape functions $k_{m,n}(X^m, X^n)$, (where $m \neq n$ and $m, n \in \{1, \dots, M\}$) are still interpretable with a heatmap on the two dimensional X^m, X^n -plane. Also, results from Lou et al. not only show that GA²M-models have a high improvement in accuracy over GAM-models, but also compete with high complexity-models in most applications.

$$g(X) = \beta_0 + \sum k_j(X^{(j)}) + \sum k_{m,n}(X^{(m)}, X^{(n)}) + \epsilon \quad (12)$$

We make use of bagging, referred to as "inner bags" in the EBM package. At the time of improving the current loss with one individual variable or interaction, the algorithm fits multiples trees on subsamples (drawn with replacement) from the training data. These trees are averaged out to create the final update of the iteration. This is proven to increase both predictive performance and interpretability of the shape functions.

To further ensure both smoothness of the shape functions and reliable estimates, EBM makes use of an outer bagging process. We refer to the hyperparameter name of its package "outer bags". What it essentially does is it fits individual EBMs on different subsamples of the training data. The final

shape functions are an average of the shape functions learned in each outer bag.

There are several approaches to detect the best set of variable interactions for our model as in [12], [9], [17], [28]. These methods however are either computationally inefficient or almost even infeasible with high-dimensional data. Therefore, we use the "FAST" approach by Lou et al. [18], which are also available in the EBM-package.

FAST's structure is based on a greedy forward stagewise selection strategy. It can be compared to the MRMR in a way that it starts with an empty set of selected pairs and an unselected set containing all possible variable pairs. In each iteration all possible unselected pairs are used separately to fit the current objective loss function resulting from the additive model including only the already selected pairs. The pair with the highest loss improvement is selected in that iteration. The iteration stops, when the objective loss function stops improving for any other inclusion of a pair.

If we assume that we have M variables in our data the amount of possible pairwise interactions equals $\binom{M}{2} = \frac{M(M-1)}{2}$. As a result, calculating the set of interaction functions and fitting all possible new models in each iteration is very time consuming for large M . FAST therefore builds the interaction functions more efficiently by defining optimized quadrants in the space of the two variables and taking the mean values of each quadrant.

The FAST algorithm is performed for each outer bag. Because there are so many interactions, we end up throwing away all but the top I interactions, where k is the number of interactions specified by the modeler. Ranking of the interactions is made by adding the loss improvement of each interaction over all outer bags.

EBM also offers hyperparameters to tune. Table 4 lists them and the value spaces used for finding the optimal hyperparameter set.

	Hyperparameter	Grid Search Values
Boosting	Learning rate λ	$\sim U(0.009, 0.015)$
	Maximum number of rounds	5000
Single Tree	Max number of tree leaves	$\sim U(2, 5)$
	Min number of samples for new leaf	$\sim U(2, 5)$
Other	Number of interactions	$\sim U(5, 10)$
	Number of Outer Bags	$\sim U(20, 30)$
	Number of Inner Bags	$\sim U(20, 30)$

Table 4: Hyperparameter sets for M-HPTL - EBM

Like for GBT, we apply an early stopping criterium evaluated on the validation set, which terminates boosting when the loss function does not improve for 30 rounds.

Again for EBM, in each iteration and for each model-HP of M-HPTL we randomly sample from the corresponding distribution/set from table 4. We apply cross-validation on the training data for generalizability. For EBM we only sample 10 times from the presented sets. The authors of EBM suggest that EBM does not need to be tuned as much as GBT in terms of model-hyperparameters. In combination with 3-fold cross-validation this totals 30 fits resulting from the M-HPTL. The best set of hyperparameters and its corresponding fit are presented as a candidate model for the current iteration of S-HPTL.

The HP-Sets for the S-HPTL we use for EBM are summarized in table 5. The same logic for the notations and abbreviations from GBT’s table 3 applies here. As custom-loss functions are not applicable with EBM we only have two sets of HPs for the S-HPTL.

	Set
Sampling	[N, d, d0.1, d0.5, u, u10, u50, sm]
Variables	[with_quot, no_quot]

Table 5: Hyperparameter sets for S-HPTL - EBM

So in total we have $8 \times 2 = 16$ iterations in S-HPTL, which decreases the computational complexity of finding the ideal preprocessing configuration. Combined with the 3-fold cross-validation we end up with $16 \times 10 \times 3 = 480$ models fitted for EBM in total. Even though this is way less than the amount of GBT models fitted, "lightgbm"'s training time is still able to outperform EBM for the entire S-HPTL and M-HPTL. This is as a major drawback of EBM. Especially when the model is operationalized for predicting customer churn in a way that it is retrained in constant time intervals.

3.6 Model Evaluation Metrics

To get an unbiased estimate of the generalized performance of our model, it must be tested on unseen data, which was not part of the training process. In order to especially ensure time generalizability of our models, we not only use out-of-sample but also out-of-period unseen data (test set) to generate evaluations.

For the evaluation of classification models there is a large variety of metrics. As already stated, selecting the correct metric is crucial. Let us first define the possible outcomes of our model with the confusion matrix:

	$\hat{C} = 0$	$\hat{C} = 1$
$C = 0$	# True Negatives (TN)	# False Positives (FP)
$C = 1$	# False Negatives (FN)	# True Positives (TP)

Table 6: Confusion Matrix

Using accuracy ($TN + TP/N$) leads to unreliable estimates of the performance with rare events. The accuracy is high indicating a good fit, even if the churners are not frequently detected. Therefore it makes sense to either use the precision ($TP/TP + FP$) or the recall ($TP/TP + FN$) metrics. A combination of both measures is provided by the F1-score which is the harmonic mean of both

metrics and therefore still defined between 0 and 1 [36]:

$$F1 = \frac{2 * precision * recall}{precision + recall} \quad (13)$$

Another widely used metric is the area under the receiver-operating-characteristic-curve (AUROC). The ROC-curve represents the tradeoff between the false-positive-rate ($FPR = FP/FP + TN$) on the X-axis and recall on the y-axis of a classifier using different cutoff values τ .

The ROC always starts at the lower left-hand corner ($FPR = 0$, $Recall = 0$) for $\tau = 1$ and ends at the upper right-hand corner ($FPR = 1$, $Recall = 1$) for $\tau = 0$. The other values of the curve are defined by alternating τ in values between 0 and 1. An area under the curve of 1 is the best score and 0.5 is the worst, representing the classifier-results of a simple coin-flipping algorithm.

This measure also has its downsides with very small positive classes, as the FPR is highly dependent on the number of negatives. The FPR only improves by a small amount if there is a substantial decrease in FPs as the number of TNs is very high for most τ 's.

For a small number of positive samples, it makes more sense to look at the area under the precision-recall-curve (AUPRC) [1]. There, the curve also plots values for the recall on the X-axis and precision on the y-axis for different τ s. It now starts at the upper left corner ($Recall = 0$, $Precision = 1$) for $\tau = 1$ and ends in the lower right corner ($Recall = 1$, $Precision = 0$) for $\tau = 0$.

Now when it comes to interpreting the metric, it is not as easy as the AUROC. The baseline now is not a simple coin-flip, but instead defined by the ratio of churners ($\#C/N$) in the data. Every AUPRC score above that baseline is an improvement from predicting customers as churners randomly using a Bernoulli-distribution for each ($C_i \sim B(\frac{\#P}{N})$).

For calculating the AUROC or the AUPRC there are multiple possibilities. All of them rely on estimates, as the true function of the curve can only be approximated using a finite number of cutoff values τ .

When comparing our model candidates, we provide all presented evaluation metrics. The ones however which are weighted the most in this application due to the presence of class imbalance are the F1-Score and the AUPRC.

3.7 Explainability of the Models

One of the main tasks of this work is to interpret the structure of our models. More precisely, we want to know how each variable interacts with the probability of an estimated churn. Especially the usage of quotation data turns out to have high predictive power, but we want to check if the assumed relationship is true and how the shape of the relationship in our models really looks like. This question is also answered for other variables which turn out to have high predictive importance in our model.

EBM is interpretable in the functional form of the individual shape functions. Therefore, we focus on explanation approaches for our black-box model of GBT. While presenting the results in the next chapter, we check if the findings and interpretations are in line with each other in both models.

For a complex model such as gradient boosted trees the model structure struggles to explain itself. Therefore, the current literature relies on simple explanation models, which are defined as interpretable approximations of the original model and either explain the average behavior of the model (global model-agnostic methods) or individual predictions (local model-agnostic methods). We shortly summarize and apply three most used methods PDP (Partial dependency plots) [7], LIME (Local Interpretable Model-agnostic Explanations) [25] and SHAP (Shapley Additive explanation) [19].

(i) Partial Dependency Plots

Partial dependency plots (PDP) ([7] and [22]) are essentially part of the global model-agnostic methods. They show the marginal effect one variable has on the predicted outcome of the model. Thereby the plot can illustrate the shape of the relationship. In a linear regression model for example, the PDP would therefore also show a linear relationship.

The partial function $\hat{f}_{PD}(X^{(j)})$ for any variable $X^{(j)}$ is then typically calculated as averages over the training data and looks like this:

$$\hat{f}_{PD}(X^{(j)}) = \frac{1}{N^{train}} \sum_{i=1}^{N^{train}} \hat{f}(X^{(j)}, X_i^{(-j)}) \quad (14)$$

So the partial function corresponds to the average marginal effect on the prediction for given values of $X^{(j)}$. Thereby $X^{(-j)}$ represents a variable matrix including all variables except $X^{(j)}$. So $X_i^{(-j)}$ are actual variable values observed in the training set and are set as inputs in combination with the corresponding value of $X^{(j)}$ into the fitted model.

The advantage of PDP is its intuitiveness and fairly easy computation. If the assumption of no correlation between the explanatory variables is met, then the interpretation is clear. The plot shows how the mean prediction of the model varies when $X^{(j)}$ changes, given the training set. Under this assumption the interpretation of a causal relationship can be made as well, as the model explicitly outputs the outcome as a function of the input.

One big disadvantage of PDP occurs if there is correlation among the variable $X^{(j)}$ and any variable(s) in $X^{(-j)}$. The averages of the calculated predictions for the partial function then include data points which are very unlikely to stem only from the variable $X^{(j)}$. In real world settings it is almost surely unrealistic to assume no correlation among explanatory variables. In our case we intentionally include highly correlated quotation variables. We try to filter for the optimal variable per variable group while considering correlation with the variable selection algorithm MRMR. After filtering however, the input matrix X still contains correlated variables. Therefore, we need to pay attention to not falsely conclude causal relationships between outcome and explanatory variable in PDP.

(ii) Local Interpretable Model-agnostic Explanations

LIME was developed by Ribeiro et al. [25] and is a local model-agnostic method. Its main goal is to understand why the fitted black-box model makes a certain prediction. Therefore, it tests what the model predicts when it is fed with variations of the original data point. This approach only relies on the data point of interest and the black-box model and does not need the entire original dataset for explaining the model.

So initially, a new dataset is needed. In this synthetic dataset the explanatory variables correspond to samples drawn near the original data point and the target variable being the associated prediction the black-box model would return. This new dataset is then used to fit an explainable model, typically a regression model with a lasso penalty. This is done, as regression models are

easily interpretable in its coefficients. While fitting the model, the synthetic data points are weighted by their similarity to the original data point of interest. It is important to note, that the regression model should be a good approximation of the black-box model locally and not globally (see [22]).

To summarize, LIME essentially consists of the following steps:

- (1) Select data point of interest
- (2) Create synthetic data points
- (3) Compute weights for new data points based on their similarity measure
- (4) Fit weighted lasso regression model on synthetic data set
- (5) Explain prediction by interpreting the coefficients

Step 2 is performed for each variable individually. So, for each variable and for every synthetic data point a value is drawn from a sample distribution of the variable. Typically, one uses normal distributions for continuous variables and bernoulli or multinoulli distributions for categorical variables. The parameters of the respective distribution are estimated with their sample-counterpart using the training data.

(iii) Shapley Additive Explanation

SHAP is a local model-agnostic method but can also be used to estimate global explanations. SHAP’s theoretical foundation originally lies in the shapley values from Game Theory [27]. To understand the approach of SHAP it is necessary to understand the computation of shapley values in a machine learning setting first. That is why the first part of this section is dedicated to an introduction into shapley values.

To link the game theoretical approach to machine learning, a prediction can be explained by assuming that each variable value of the sample is a “player” in a game where the prediction is the “payout”. The shapley values then tell us how to fairly distribute the “payout” among the variables.

The goal of shapley values in the machine learning setting is to explain each variable’s contribution to the specific outcome. More specifically, a shapley value computes the contributions to the estimated deviation to the mean of the output variable (in our application: $\hat{C}_k - \frac{1}{N} \sum_{j=1}^N C_j$). We denote $\delta^{(i)}$ as the contribution of variable i to the particular prediction compared to the average value of the outcome variable, or in short the shapley value.

The shapley value is estimated by the average marginal contribution of a variable value across all possible coalitions with the other explanatory variables. To elaborate what is meant by all possible coalitions we provide an example model consisting of 3 explanatory variables $X^{(1)}$, $X^{(2)}$, $X^{(3)}$. Let us assume that for a given sample i , outcome $\hat{Y}_i = 0.4$ is predicted using variable values $X_i^{(1)} = 10$, $X_i^{(2)} = 15$ and $X_i^{(3)} = 5$. The average predicted value for the output variable is say $\bar{Y} = 0.5$. We further assume, that we want to calculate the shapley value $\delta^{(1)}$ of $X_i^{(1)} = 10$, which is the average marginal contribution of that variable value to \hat{Y}_i having an 0.1 deviation to its average. To do this we form all possible coalitions with $X^{(1)}$:

- (1) No variable values
- (2) $X_i^{(2)} = 15$
- (3) $X_i^{(3)} = 5$
- (4) $X_i^{(2)} = 15$ & $X_i^{(3)} = 5$

For each of these coalitions we compute the estimated \hat{Y}_i (1) with and (2) without $X_i^{(1)} = 10$. The difference between (1) and (2) represents the marginal contribution. The shapley value $\delta^{(1)}$ is the average of all marginal contributions. If a variable value is not included in a coalition a variable value is randomly picked from the training data to represent the mean of that variable. To have more reliable estimates of $\delta^{(1)}$, sampling and the computation of marginal contributions is repeated multiple times (M) and averaged at the end.

The computation time of shapley values rises exponentially with the number of variables due to the exponential relationship with the number of coalitions. This is a disadvantage of shapley values in general. This creates a trade-off between accurate predictions of marginal contributions (high M) and fast computation time (low M). Several methods are being developed at the moment to define the optimal M to maintain low variance in the estimates for $\delta^{(i)}$ and low computation time (see [22]).

SHAP, developed by Lundberg et al. [19], has a slightly different approach in estimating the shapley values. Its innovation lies in the shapley value explanation being represented as an additive variable attribution method, a linear model. Regarding this aspect SHAP and LIME have similarities. The linear model can be specified as:

$$g(z) = \delta^{(0)} + \sum_{j=1}^M \delta^{(j)} z^{(j)} \quad (15)$$

where $z \in \{0, 1\}^M$ is a vector defining the coalition form, M is the maximum coalition size and $\delta^{(j)}$ is the shapley value of variable j . The vector z therefore serves as a collection of explanatory variables in the linear model and defines if variable j is present in the coalition or not. So if we take the example from above, a vector $z = [1, 0, 1]$ would represent the coalition of $X_i^{(1)} = 10$ and $X_i^{(3)} = 5$. $g(z)$ would represent the model output for $X_i^{(2)}$ being drawn from the training data.

Similarly to LIME, in the first step a synthetic dataset for the sample of interest is computed using different vectors z . The dataset then consists of the coalition vectors and their corresponding model estimates $g(z)$. Again, as we aim to minimize the variance of the shapley value estimates, for each coalition vector we sample M times (unless z is a vector of 1s). With this new dataset we try to fit the simple linear model in equation (15). The shapley values are the coefficients of the model which are typically estimated by kernel methods.

The big advantage of SHAP over the normal computation of shapley values is the ability to efficiently compute the shapley values estimates for all variables at once. Also, with this simplified estimation it is possible to go from local to global interpretations. We shortly describe two methods which can be used to illustrate global effects of variables.

The first method is named SHAP variable importance and is easy to compute. It neglects the direction in which a variable affects the model output, however it is a powerful way of measuring average absolute effects of the variables. This is essentially what is performed to get the desired SHAP variable importance, as we average over the absolute shapley values per variable across the data:

$$I_{SHAP}^{(j)} = \frac{1}{N} \sum_{i=1}^N |\delta_i^{(j)}| \quad (16)$$

The second method does not rely on any further computation and simply visualizes the shapley values for all variables and for every sample. It is therefore

named SHAP summary plot. Even though there is no new metric behind its representation of global explanation, the method is still powerful and interpretable. The plot is constructed in a way such that each point represents one shapley value for a variable and a sample. Therefore, one axis lists the variables whereas the other corresponds to the shapley value. An additional way to make the resulting plot more interpretable is to add a third dimension, representing the variable value, in form of colors. To get an idea on how SHAPs summary plot looks like we refer to figure 12.

To summarize, we present methods used in this work to successfully model the underlying problem of customer churn. This chapter deals with all steps of the machine learning pipeline, starting with preprocessing the data, dimension reduction and the methods to handle class imbalance. We illustrate the mathematical and statistical foundations behind the two models, their evaluation and interpretation methods. We are now well equipped to apply these methods evaluate and compare them to build the best prediction model.

4 Results

In this chapter we present the results of our modelling approaches. First, we give short insights into the data set structure after data preparation. Then we present two baselines for which we aim to improve on. GBT and EBM differ slightly in their modelling structure. Therefore, we split the result presentation in two parts and examine them separately in terms of improvement to the baselines. As this work focuses both on evaluation of the model’s predictive performance and its interpretability, we compare both GBT and EBM in both areas in the last section of this chapter.

4.1 Exploratory Data Analysis

We again shortly note that the data used to show the modelling results are based on a toy data set. Due to data protection law it is not possible to publish real data from customers. The toy data however is constructed in a way that it includes key variables, metrics and relationships of the true data. We exclude the latest period of the resulting data set ($N = 110,000$) as an

out-of-period data set ($N = 10,000$). The other fraction ($N = 100,000$) is used for training, validation and out-of-sample testing, where for both GBT and EBM we perform the same split of 80/10/10. The split stratifies for the target variable "churn", so proportions of churners are approximately equal in all three subsets. The entire toy data undergoes the same data preparation steps described in chapter 3.1.

High class imbalance is present just as in the real data, as churners only make up around 1% of the data. We have 20 variables besides the churn status. 12 of them are generated through the quotation data. Remember that we only keep 4 of them after dimension reduction, representing the best m per quotation variable group. The rest of the variables contain either contract or car related information. How these variables are exactly named and how they are distributed for each churn status $C \in \{0, 1\}$ can be observed in the violin plots of figure 6 and 7.

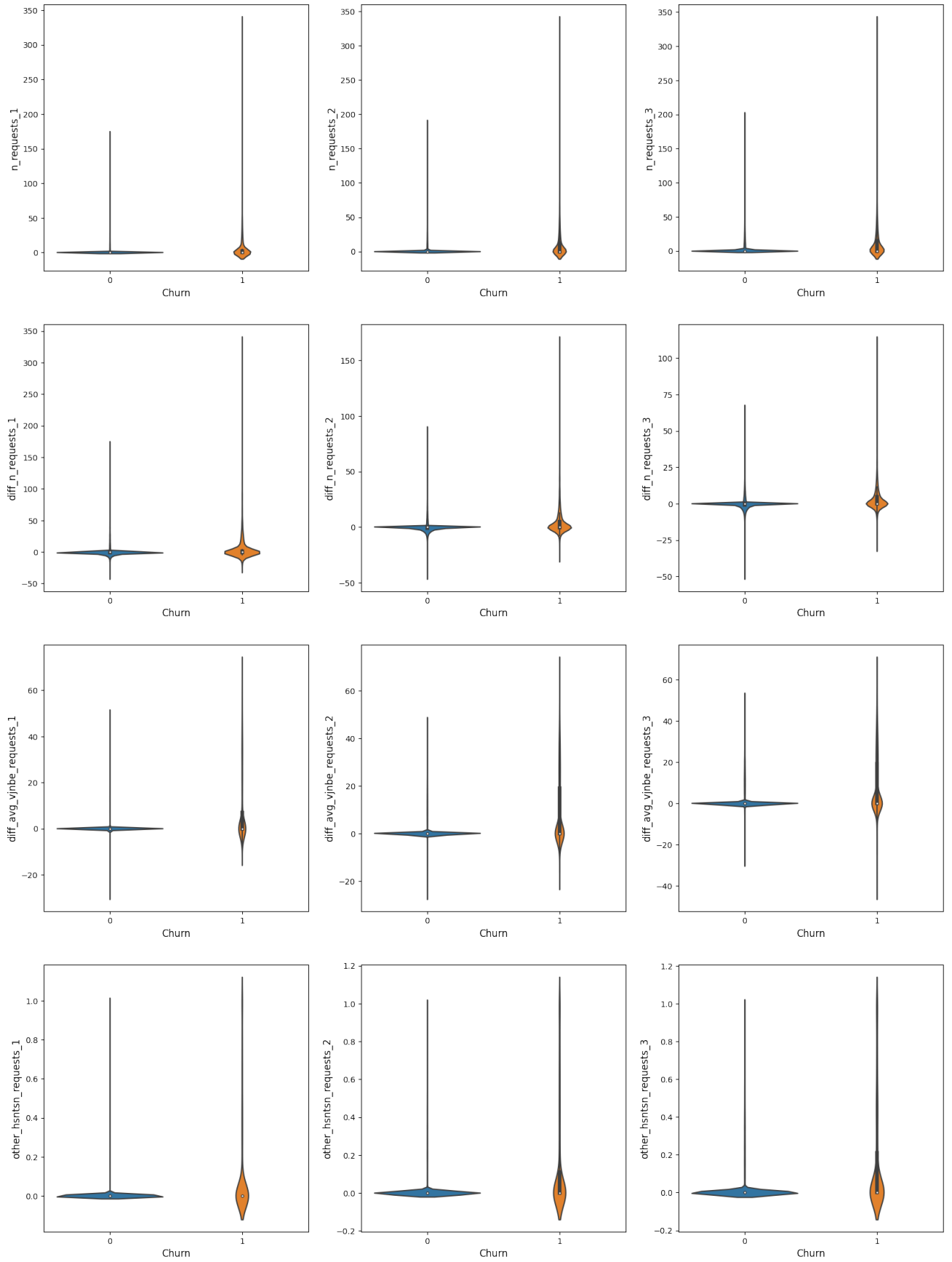


Figure 6: Violinplots for Quotation Variables

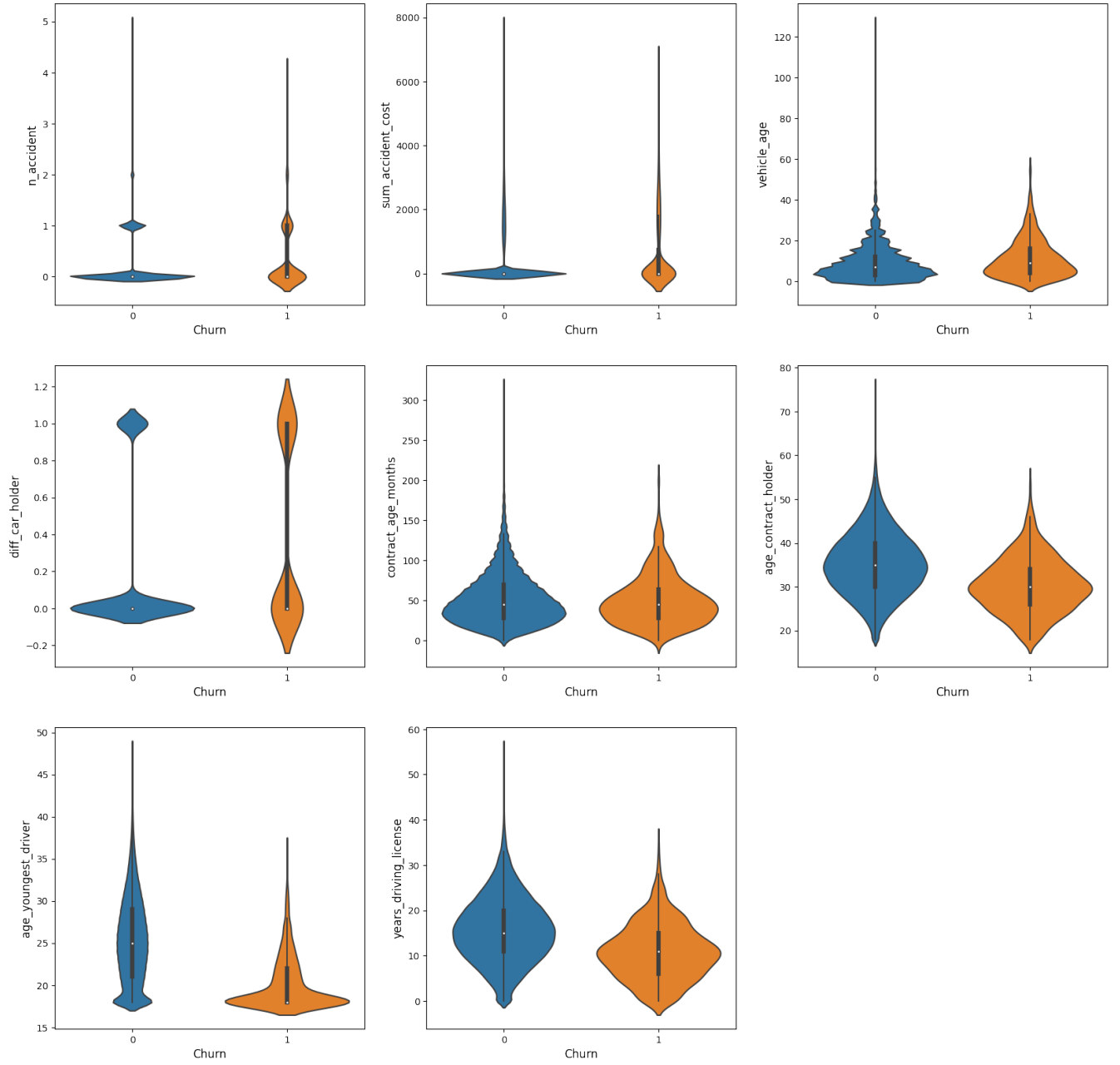


Figure 7: Violinplots for Non-Quotation Variables

The key insights that are generated through exploring the data point at the effectiveness and importance of including quotation data in churn modelling.

(1) There are significant differences in the averages and the standard deviations (the distribution in general) in the number of requests generated 1, 2 and 3 months before t , when comparing the group of churners with the group of non-churners. The relative difference is the highest for "n_requests_1", with an average of 0.96 for non-churners versus 6.26 for churners, and a standard

deviation of 6.15 versus 18.32.

Note that the distribution is heavily right skewed, which is represented by the median being 0 for both groups. This indicates that the majority of customers, for both customers with and without a willingness to churn, do not generate requests.

Other key insights include but are not limited to the following: (2) The average (and standard deviation) of "diff_n_requests_1" with 4.95 (and 18.54) for churners is also significantly larger than 0.01 (and 6.45) for non-churners. This reflects that the request behavior of customers which are about to churn changes significantly, while non-churners show the same behavior.

(3) The average calculated price for churners was significantly higher than the price they are paying in their contract. This is reflected in the means of "diff_avg_vjnbe_requests_1" with a difference of 15.00. For non-churners this difference is also positive but only around 20% as high.

(4) A proportion of churners do search for different cars than their current car in their request. This is reflected by the average of "other_hsntsn_requests_1" for churners being 0.10. This average is smaller for non-churners with 0.01.

(5) Regarding non-quotation variables, most noticeable are the significantly lower averages and medians for churners in terms of the age variables, especially "age_youngest_driver".

4.2 Modelling Baseline

To get an idea on how well a specific model is performing it is useful to have a baseline for the evaluation metrics. Typically, the baseline is a simple model/solution. When applying a new solution to solve a business problem, stakeholders are predominantly interested in the generated improvement in terms of profit (or other business KPIs). Therefore in this context, the status quo is selected as the baseline in most cases. Whether the solution achieves an improvement over the status quo is decisive for the implementation of it.

In the application of this work, the status quo consists of the no-existence of any mid-contract-period churn prediction model. The fact that quotation data availability and quality was ensured only a few months before this work is the reason for it. As this work underlines the importance and predictive power of quotation data in churn contexts, earlier attempts of modelling this problem were unsuccessful.

Hence, the most naïve baseline we can set for our modelling is that mid-contract-period churns are never predicted. We name and index this baseline with "B1". Applying this rule to compute the confusion matrix both on the out-of-sample (OOS) and out-of-period (OOP) test data, we are left with following results:

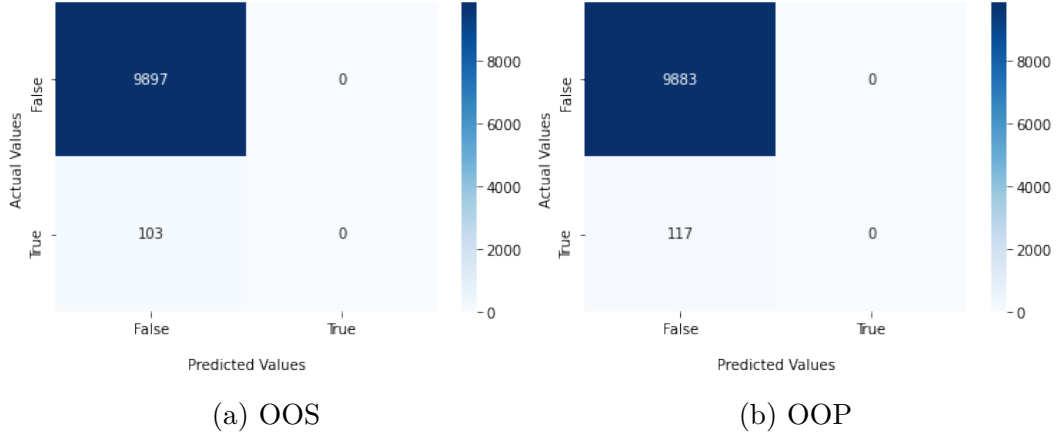


Figure 8: Baseline 1 (B1); Status Quo

We introduce another baseline which is based on a simple decision rule. This decision rule leads to a prediction of churn if the specific customer showed quotation activity in the past month. This implies:

$$\widehat{C_{t+s}^{class}} = \begin{cases} 1, & \text{if } n_requests_{t-1,t} > 1 \\ 0, & \text{if } n_requests_{t-1,t} = 0 \end{cases} \quad (17)$$

The resulting confusion matrices for OOS and OOP from this baseline (B2) are plotted in figure 9.

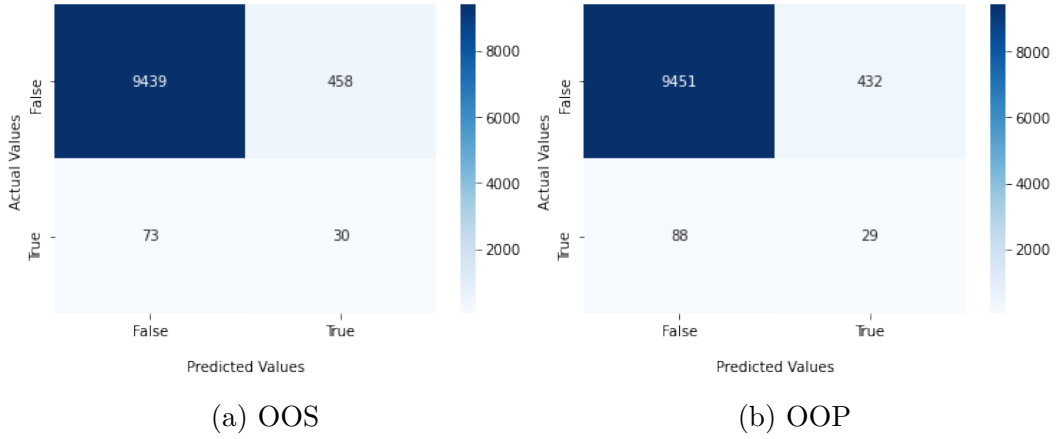


Figure 9: Baseline 2 (B2); Quotation Activity

We further summarize all evaluation matrices for B1 and B2 we are interested in and we want improve on with our modelling approach in table 7.

	Accuracy	Precision	Recall	F1	AUROC	AUPRC
B1 on OOS	0.9897	0.0000	0.0000	0.0000	0.5000	0.0103
B1 on OOP	0.9883	0.0000	0.0000	0.0000	0.5000	0.0117
B2 on OOS	0.9469	0.0615	0.2913	0.1052	0.6225	0.0252
B2 on OOP	0.9480	0.0629	0.2479	0.1003	0.6021	0.0244

Table 7: Baseline Evaluations on Test Data

4.3 Modelling Results

While presenting the results we want to emphasize, that for both modelling approaches GBT and EBM we use figure 5 representing one iteration of the Structural-HP-Tuning-Loop (S-HPTL) as the modelling structure. The Model-HP-Tuning-Loop (M-HPTL) and the Structural-HP-Tuning-Loop (S-HPTL) are in depth explained in chapter 3.2. During M-HPTL, for each hyperparameter we sample from the corresponding set presented in table X for GBT and from table Y for EBM.

We of course do not present each of the fits performed in the inner loop (M-HPTL). Remember, that the M-HPTL nests in each iteration of the S-HPTL, which further increases the number of total fits. Therefore, we focus only on the

M-HPTL optimal result, which is essentially one best model-hyperparameter set, its trained model and its evaluation scores.

(i) Gradient Boosted Trees Results

Before presenting the results, we want to make some additional notational remarks. We denote the best model resulting from M-HPTL for a specific iteration of S-HPTL by: "gbt_{sampling method}_{custom loss parameters}". So for example "gbt_d0.1_a0.6g2" represents the best model with a downsampled dataset with factor 0.1 and with a focal loss implementation of $\alpha = 0.6$ and $\gamma = 2$. Also, for now we concentrate on the models fitted including the best set of quotation variables. This is why this notation does not include an indicator for which variables are used. With the best model at hand however we compare both with and without quotation variables results in order to show the importance of them.

Moreover, we do not present the resulting best model from each S-HPTL iteration, as we have $8 \times 4 \times 6 \times 2 = 384$ iterations in total. We focus on the main insights and present the best results in terms of evaluation metrics in table 8.

First insights which are generated through looking at the results are the following:

- (1) The out-of-period evaluation scores for almost all models are lower than the ones for out-of-sample. This holds true for almost all applications and was expected. As churn rates differ from period to period, we intentionally raised the number of churners by 10% to also evaluate robustness over time of the model candidates.
- (2) Sampling towards a balanced training data set in general creates confidence in the model to predict the minority class. This is reflected in a dropping precision and a rising recall.
- (3) Even though SMOTE is said to be a more advanced and reliable approach than upsampling, the latter yields better results in our application.
- (4) Using weights α in the loss functions delivers same results to sampling in terms of confidence. Additionally with a too high α (starting at $\alpha = 0.7$) the F1-Score and the AUPRC start to drop.
- (5) Adding $\gamma \neq 0$ to the loss, we also observe confidence in the model, but this confidence is not restricted towards predicting the minority class. Paired

Model	Test-Set	Accuracy	Precision	Recall	F1	AUROC	AUPRC
gbt_u10_aNgN	OOS	0.9857	0.3246	0.3592	0.3410	0.8782	0.3231
	OOP	0.9843	0.2727	0.2051	0.2341	0.8438	0.1909
gbt_d0.1_aNgN	OOS	0.9790	0.2390	0.4757	0.3182	0.8921	0.3267
	OOP	0.9767	0.1947	0.3162	0.2410	0.8485	0.2070
gbt_u_aNgN	OOS	0.9162	0.0761	0.6408	0.1361	0.8791	0.3310
	OOP	0.9126	0.0733	0.5556	0.1295	0.8389	0.1956
gbt_d0.1_a0.6gN	OOS	0.9702	0.1803	0.5340	0.2696	0.9032	0.3338
	OOP	0.9645	0.1234	0.3333	0.1801	0.8577	0.1924
gbt_u_a0.8gN	OOS	0.8487	0.0487	0.7379	0.0913	0.8746	0.2972
	OOP	0.8378	0.0442	0.6239	0.0826	0.8251	0.1923
gbt_u50_aNg0.5	OOS	0.8970	0.0530	0.5340	0.0965	0.8452	0.0498
	OOP	0.8884	0.0463	0.4360	0.0837	0.8045	0.0385
gbt_sm_aNg2	OOS	0.8285	0.0462	0.7961	0.0873	0.8808	0.1267
	OOP	0.8157	0.0405	0.6496	0.0762	0.8293	0.0732
gbt_u50_a0.6g1	OOS	0.8973	0.0471	0.4660	0.0855	0.7909	0.0340
	OOP	0.8872	0.0433	0.4102	0.0784	0.7786	0.0324
gbt_sm_a0.7g2	OOS	0.5378	0.0196	0.8932	0.0383	0.8074	0.0397
	OOP	0.5237	0.0208	0.8632	0.0406	0.7864	0.0358

Table 8: Evaluation of GBT-Candidates on Test Data

with a low α a too high γ (> 1) can have backfiring effects and lead to no predictions of the minority class. When a too high γ is paired with a high α however, the model fit can lead to only predicting the minority class. The main takeaway for the usage of focal loss is to carefully select the parameters, as with wrong calibration it can lead to overconfidence.

(6) Even though using a cost-sensitive loss function is highly suggested in the literature, standard sampling methods alone or paired with a cost-sensitive loss yield better and more robust results in our application.

Best GBT model candidate

Due to the high class imbalance, the main evaluation metrics we look at in this work are the AUPRC and the F1-Score. There is no candidate which scores highest in both metrics. Nevertheless "gbt_u10_aNgN" has by far the highest F1-Score and only lacks a small amount behind other candidates in terms of AUPRC. Therefore, the model that represents our best GBT candidate is obtained with an upsampled ($\times 10$) minority class and no cost-sensitive loss function. "n_requests_1", "diff_n_requests_3", "diff_avg_vjnbe_requests_3" and "other_hsntsn_requests_3" are used as the optimal quotation variable set resulting from MRMR dimension reduction.

The trained model yields a 224% (and 133%) improvement in the F1-Score on OOS (and OOP) data over the Baseline 2. The increase in AUPRC on OOS (and OOP) data for B2 amounts to 1182% (and 682%).

"gbt_u10_aNgN"'s evaluation scores are much higher with the best set of quotation variables than without, which highlights its predictive power. The absolute deviation of the F1-Score without quotation variables on OOS data lies at -0.2234 , for OOP at -0.1267 . The AUPRC is 0.2515 lower for OOS data and for OOP 0.1342 lower. This fact also holds true for all other GBT candidates. Table 11 in the appendix summarizes the gain in the evaluation metrics generated through the inclusion of quotation data for all candidates.

Interpretation of GBT candidate

We use "gbt_u10_aNgN" to shed light on this black box in order to make it interpretable. Therefore, we make use of explainability methods PDP and SHAP. Both methods are explained in chapter 3.7.

Figure 10 presents the PDP's for the main drivers behind this model. The first graph represents the PDP for variable "n_requests_1" and confirms the hypothesis of a strong positive relationship between it and the probability of a churn. The relationship shown for "diff_n_requests_3" is also as expected, the higher the difference of quotation activity to the normal behavior the higher the probability of a churn. The insights generated through the PDPs for the remaining two quotation variables do not show the expected relationship. This however can be caused by the disadvantage of PDP's when facing correlated explanatory variables.

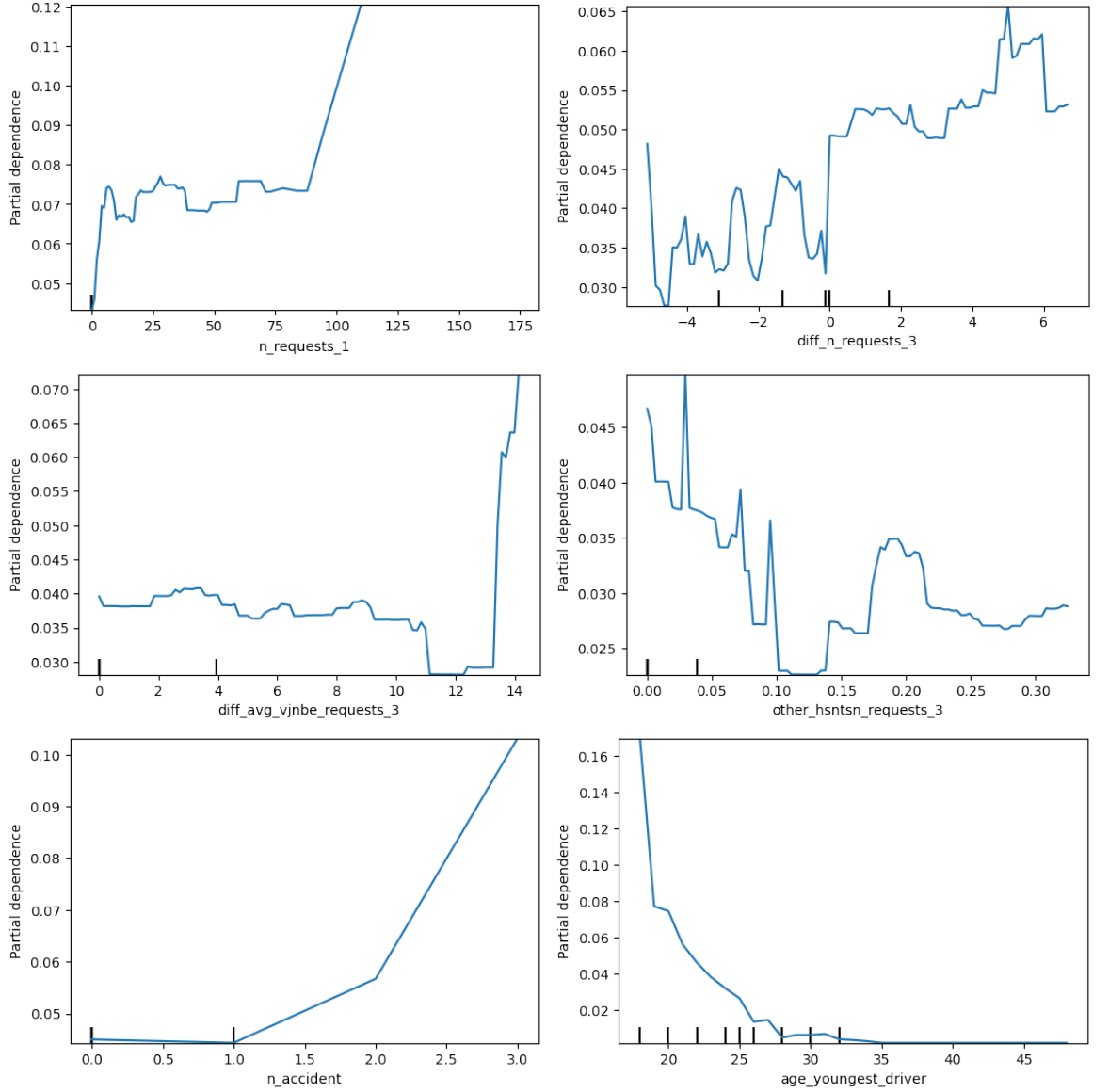


Figure 10: Partial dependency plots (PDP) for GBT

The lower two graphs show the two non-quotation variables which have the strongest relationship with the target variable. On the left we see that the number of accidents since the start of the contract go along with a higher predicted probability on average. Considering the fact, that an accident gives customers the exceptional right of mid-contract-period termination, this relationship is intuitive. More importantly, following an accident the insurer raises the insurance fee in most cases which obviously raises the probability of a churn.

The strongest partial dependency relationship is shown in the age of the youngest driver registered in the contract. The explanation for this effect may

be that driving-license-freshers are typically first registered in the insurance contract of their parents or other relatives. As a reaction insurance companies raise the insurance fee, as young drivers typically pose a higher risk for accidents. The reaction of the customer is a higher probability of churn.

Figure 12 visualizes SHAP's summary-plot, a method to transform the local model-agnostic method of SHAP to a globally interpretable one. Each dot represents one sample and the contribution of its corresponding variable value (y-axis) to the predicted log-odds (x-axis). The insights of this plot are almost all in line with the ones from PDP. Most dominant are the average contributions of "age_youngest_driver" to the log odds. It also hints at a negative relationship, the one with highest impact on the predictions, which is in line with PDP.

In this summary plot, SHAP shows new insights on the model behavior for "diff_avg_vjnbe_requests_3". More precisely, for some samples a high deviation between the average price shown during the requests and the contract fee increases the predicted probability by the most among all variable contributions.

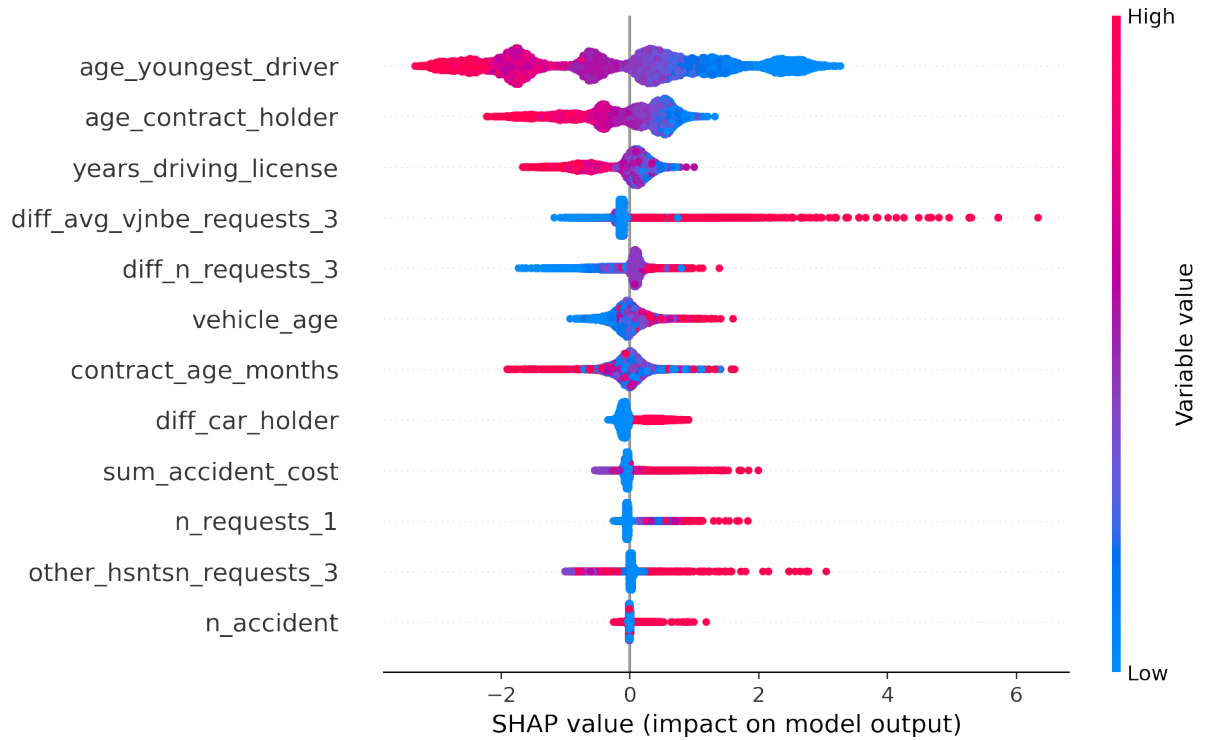


Figure 11: SHAPs Summary Plot on GBT candidate Model

The SHAP-values of a single prediction also provide good explanations of how the prediction is generated and how each variable value contributed. In our context of customer churn single explanations can be applied on predicted churners before taking any action (call customer or give rebates) to fully understand the reason of the prediction. Figure 12 shows how the SHAP-Values can be visualized. There, each bar visualizes the estimated Shapley value $\delta^{(j)}$ of the corresponding variable value. Stacking all bars on top of each other results in a representation on how the predicted log differs from the sample mean.

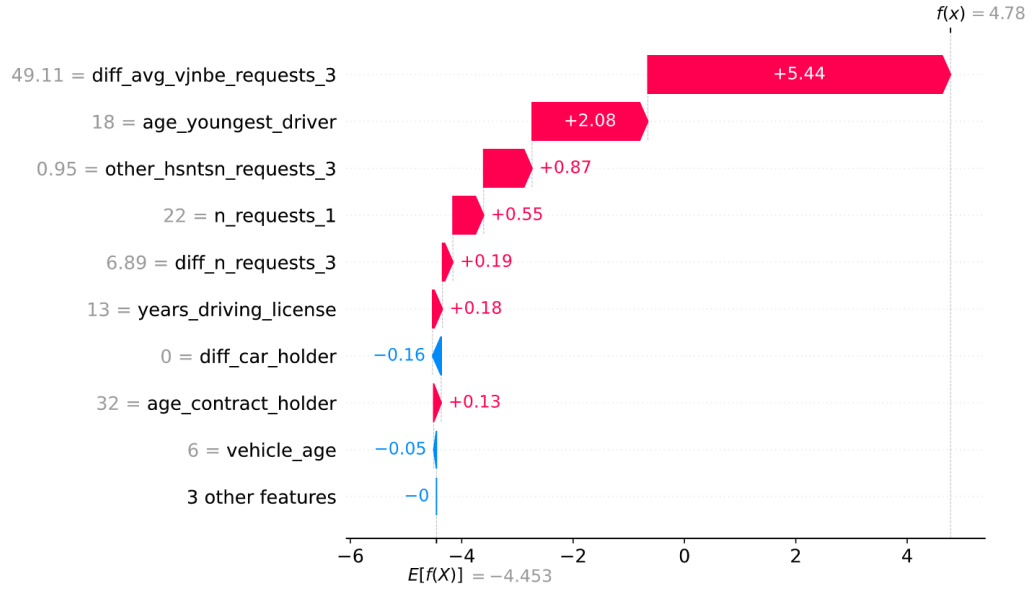


Figure 12: SHAPs Summary Plot on GBT candidate Model

In this example, the difference in the average price shown during the requests has the highest contribution to the prediction. This customer also has a young driver registered which also rises the model probability. The fact, that 95% of the requests belonging to that customer included a different car than the one in his contract, has the third highest contribution. All other variable values only have minor contributions for this example.

This concludes the result presentation of the GBT modelling approach. We present 9 candidate models, all using different sets of sampling methods, loss functions and explanatory variables. The best model turns out to be the result of an upsampling approach in combination with no cost-sensitive loss-function. The quotation data shows to have high predictive power for GBT, and we use

explainability methods to examine the relationship between prediction and the main drivers of the model. In the next section we compare these results with the EBM approach.

(ii) Explainable Boosting Machine Results

Also, regarding the best model resulting from M-HPTL for a specific iteration of S-HPTL we use a similar notation: "ebm_{sampling method}". We again first only present model performances of EBM candidates including the best set of quotation variables. With the best model at hand however we compare both with and without quotation data results in order to show the relevance of quotation data. Table 9 summarizes the best 5 models and their OOS and OOP performances.

Model	Test-Set	Accuracy	Precision	Recall	F1	AUROC	AUPRC
ebm_none	OOS	0.9912	0.8000	0.1942	0.3125	0.5968	0.1636
	OOP	0.9892	0.7647	0.1111	0.1940	0.5554	0.0954
ebm_d0.1	OOS	0.9821	0.2683	0.4272	0.3296	0.7075	0.1205
	OOP	0.9808	0.2302	0.2735	0.2500	0.6313	0.0715
ebm_d0.5	OOS	0.9911	0.6750	0.2621	0.3776	0.6304	0.1845
	OOP	0.9885	0.5294	0.1538	0.2384	0.5761	0.0913
ebm_d	OOS	0.8050	0.0412	0.8058	0.0784	0.8054	0.0352
	OOP	0.7941	0.0420	0.7607	0.0796	0.7776	0.0347
ebm_u10	OOS	0.9822	0.2582	0.3883	0.3101	0.6884	0.1065
	OOP	0.9805	0.2090	0.2393	0.2231	0.6143	0.0589

Table 9: Evaluation of EBM-Candidates on Test Data

This table delivers following insights regarding best sampling methods and comparison to GBT:

- (1) The F1-Score is comparable to - and for one candidate even higher than - the GBT candidates. The AUROC and AUPRC however are lower for all EBM-candidates.
- (2) For almost all EBM-candidates, the differences between OOS and OOP

evaluation scores are as high as for GBT.

(3) Same observations apply for EBM as for GBT in terms of sampling effectiveness and implications on evaluation metrics.

Best EBM model candidate

Looking at the AUPRC and the F1-Score, "ebm_d0.5" scores the best on the OOS set. Even though it is not the best candidate in terms of OOP evaluation, there is no other candidate which outperforms it in both metrics on OOP data. Therefore, we pick this model using a downsampled ($\times 0.5$) training data set as the best EBM-candidate. The quotation variables which survived the MRMR-filtering are also: "n_requests_1", "diff_n_requests_3", "diff_avg_vjnbe_requests_3" and "other_hsntsn_requests_3". Optimal interactions which are detected with the FAST algorithm are:

- (1) diff_avg_vjnbe_requests_3 x age_youngest_driver
- (2) diff_avg_vjnbe_requests_3 x n_accident
- (3) other_hsntsn_requests_3 x vehicle_age
- (4) diff_avg_vjnbe_requests_3 x age_contract_holder
- (5) diff_avg_vjnbe_requests_3 x years_driving_license
- (6) diff_avg_vjnbe_requests_3 x contract_age_months
- (7) diff_avg_vjnbe_requests_3 x other_hsntsn_requests_3
- (8) diff_avg_vjnbe_requests_3 x sum_accident_cost
- (9) n_requests_1 x age_youngest_driver

The trained EBM-model yields a 258% (and 126%) improvement in the F1-Score OOS (and OOP) over the Baseline 2. The increase in AUPRC on OOS (and OOP) data for B2 amounts to 632% (and 262%).

The EBM modelling approach also highlights the predictive power of quotation data in churn prediction application. Absolute differences in the F1-Score without quotation variables constitute to -0.3776 for OOS evaluation, for OOP to -0.2216 . The AUPRC is 0.1742 lower for OOS data, for OOP 0.0754 lower. This effect is also visible for all other candidates of EBM and is summarized in table 12 in the appendix.

Interpretation of EBM candidate

EBM's big advantage is its simple interpretability. The addition of the individual values from the shape functions forms the log odds. Each shape function takes at most 2 explanatory variables (2 for interactions) as input. Therefore, plotting these shape functions tells us the relationship of variable (or variable interaction) and predicted log odds. Also, because of the additive model structure, local and global interpretations are equal for EBM.

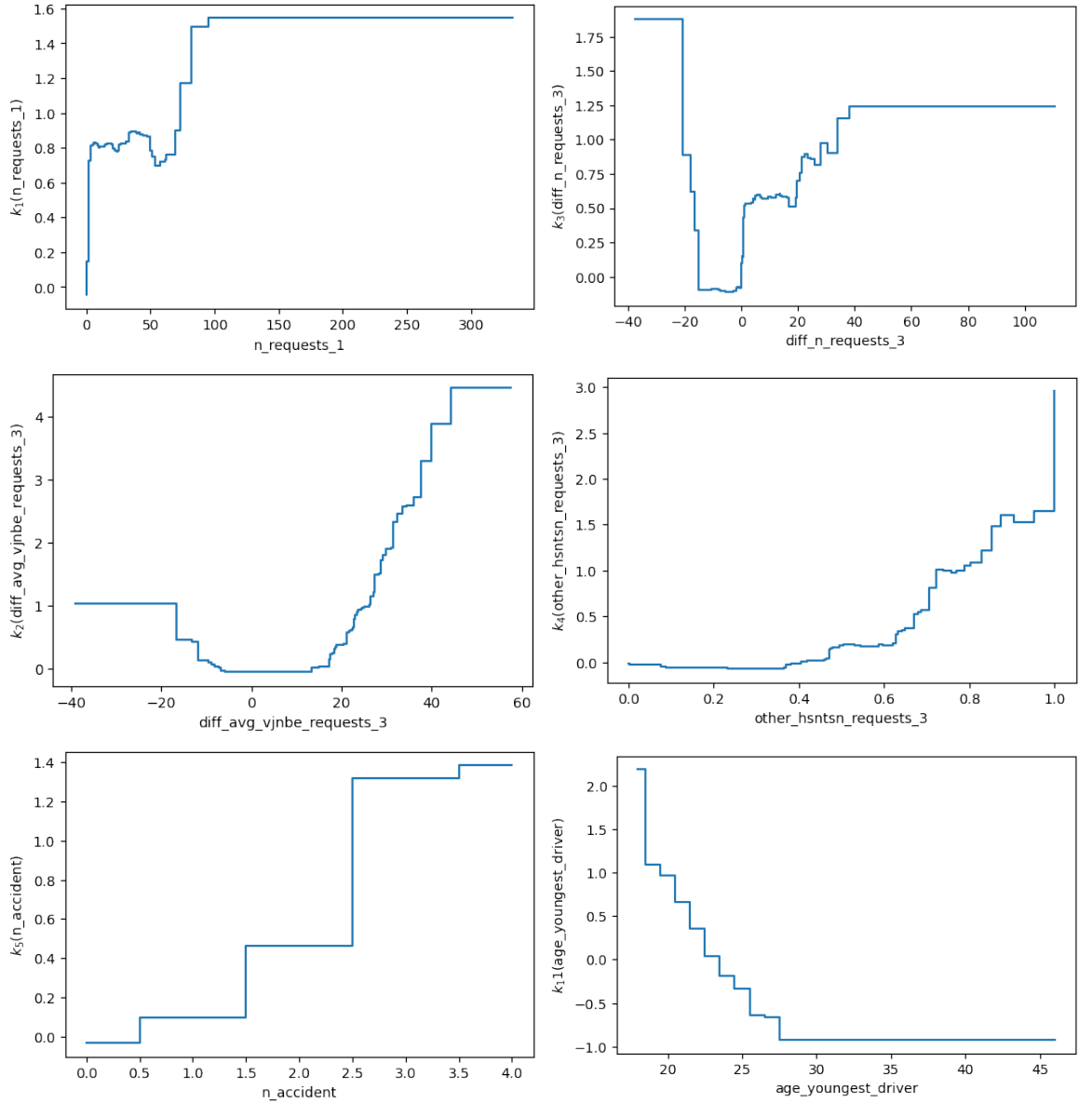


Figure 13: Shape functions of EBM

Figure 13 shows the main drivers for the best performing EBM candidate. Note that the plots should be interpreted carefully and should not be falsely compared to the PDP plots. Note, that in contrast to the PDPs for GBT, the y-axis now represents the value of the shape function. For a specific variable value, the value of the shape function is its additive contribution to the log odds.

What stands out in this figure is that quotation variables have stronger relationships with the log odds (and therefore also with the predicted probability of a churn) than non-quotation variables. This insight again strongly supports the inclusion of quotation variables for churn modelling.

Additionally, all plots show the expected behavior of variable-target relationships. For "n_requests_1" for example, the log-odds contribution rises sharply from below 0 to 0.8 for more than 0 requests. Except the drop at around 55 requests, the contribution rises steadily to 1.5 for more than 100 requests.

The plot for "diff_n_requests_3" shows the expected behavior for positive deviations, but also generates a new hypothesis for negative deviations. The peculiarity is the again sharply rising contribution at around $\text{diff_n_requests_3} = -17$. It could be explained by the phenomenon, that customers who normally have high quotation activity but did not show them in the last 3 months have already predecided to only look for other insurers before churning. This relationship is not visible with explainability approaches for GBT.

The strongest contributions to the log odds are generated by rising deviations in request-price versus contract-price and an increasing percentage of deviating car searches. For $\text{diff_avg_vjb_requests_3} = 40$ the contribution reaches a value of 4, whereas with 100% deviating car searches the contribution amounts to around 2.9.

The best non-quotation variables also show an expected relationship. "n_accident"'s contribution to the log odds rises approximately linearly from 0 to 1.4 for 4 accidents in the contract period. A negative relationship is shown by the age of the youngest driver and its contribution, until the age reaches 28. For older youngest drivers it stays stable at around -0.9.

Even though the interaction variables do not show strong contributions on the log odds, we present one example interaction of "diff_avg_vjb_requests_3" and "n_accident" in Figure 14. It is an example for how even interactions can be visualized and interpreted. All other variables and variable pairs only have a comparably weak relationship and are therefore not presented.

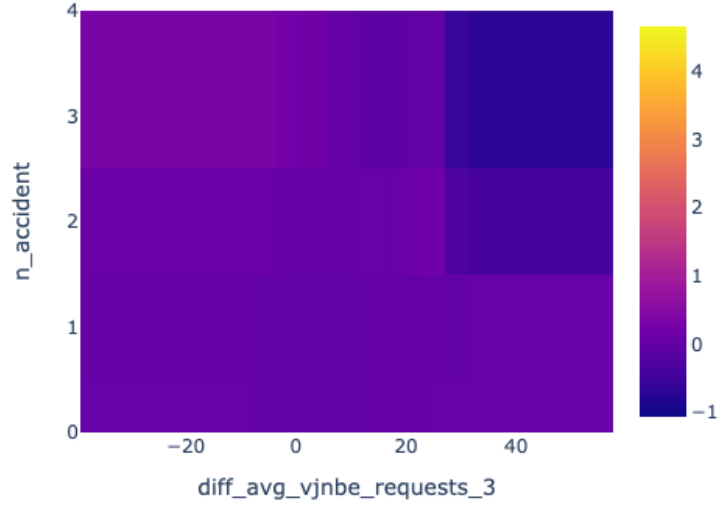


Figure 14: Relationship of Interaction Term and Log Odds

To summarize the results for the EBM approach we present 5 candidate models, all using different sets of sampling methods and explanatory variables. Downsampling the majority class by 50% and including the best set of quotation variables yields the best evaluation scores. Plots of individual shape functions enable to easily examine relationships between log odds and variable of interest. Besides confirming presumptions made for relationships, the plot give new insights. We are now able to compare both modelling approaches and simulate their improvement over the status quo, when deployed in practice.

4.4 Comparison of GBT and EBM

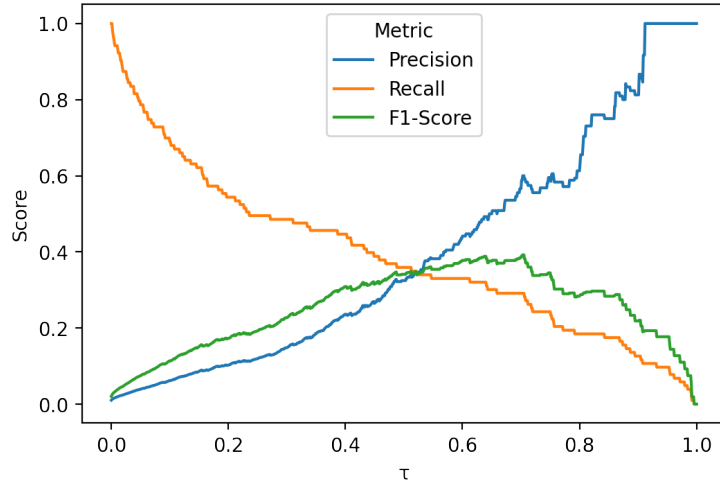
Besides showcasing the predictive power of quotation data, the goal of this work is to compare both modelling approaches in two areas. The first criterium is the evaluation (F1-Score, AUPRC) on unseen data. We also emphasize the importance of interpretability and therefore this is the second criterium. We shortly summarize which model of the two best candidates wins in each criterium.

EBM is definitely more interpretable than the explainability approaches for GBT. The shape functions are the exact explanation how a certain variable value leads to a certain increase or decrease in odds. SHAP and PDP only capture estimated relationships of EBM, which is in line with the findings of Rudin et al. [26]. Even though they help to understand the black-box model, they do not and cannot represent the exact behavior of the model. So, for

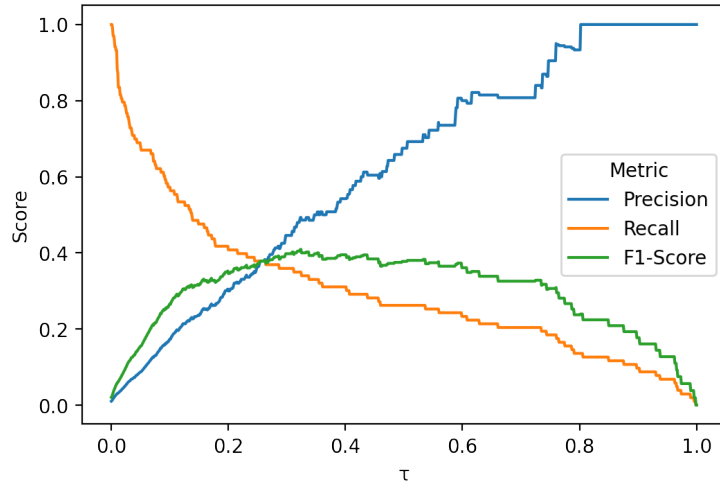
answering the question on which the main drivers for high/low churn probabilities are, EBM gives more reliable reasonings. This is reflected in the fact that PDP and SHAP could not capture all insights generated with the shape functions of EBM.

Even though EBM is not able to capture all higher order interactions relevant for the modelling problem, in our application it reaches a higher F1-Score than the GBT candidate. The AUPRC-metric however belongs to GBT, as it is almost 1.5 times as high for OOS data, for OOP almost 2 times.

The F1-Score surely depends on the selected cutoff τ , which assigns a prediction based on its probability to the two classes. We therefore evaluate Precision, Recall and the resulting F1-Score for both candidates and for 1000 different values of τ between 0 and 1 in figure 15. The lower AUPRC of EBM can be explained by low recalls and precisions for most of τ 's space. The lower F1-Score for GBT however could be caused by $\tau = 0.5$ not being the optimal cutoff.



(a) GBT



(b) EBM

Figure 15: Comparison of Candidates' Evaluation Metrics for different τ 's

The two plots in figure 15 show, that both candidates for GBT and EBM obtain almost similar evaluation scores, but for different cutoff values τ . Based on the given metrics, a decision in favor of one candidate is therefore not feasible. None of both show dominance in both highly important metrics. We want to emphasize that the comparison of both models should be made on the possible profit increase the models can achieve in the designated setting. This is why the following part will serve as a simplified exemplary simulation.

Exemplary Simulation

As in most applications, the modeler faces a trade-off when selecting the optimal model and/or the optimal τ : High precision versus high recall. How to evaluate this tradeoff typically depends on the costs of false classification on the one hand and the profit of correct classification on the other.

We therefore provide a simplified simulation for our application on the OOS data set ($N = 10,000$), in order to determine the optimal cutoff for both models. First, we define a profit-increase-function and its parameters needed. For the function we assume that the models are applied only once to predict potential churners in the subsequent two months. This can be extended to a multi-period setting, but the optimal τ stays the same. All customers are assumed to have the same net-profit-value (NPV) and all predicted churners ($N^{\hat{C}=1}(\tau)$) receive a rebate r as a churn prevention strategy. Further parameters and their assumption for the simulation are explained in the below table.

Parameter	Explanation	Value
$\Delta\Pi(r, \tau)$	Profit-Increase to Status-Quo	
$N^{\hat{C}=1}(\tau)$	Number of predicted Churners	
$p^{prec}(\tau)$	Precision of Model	
$p_i^{succ}(r)$	Probability of Rebate Success	0.9
NPV_i	Net-Profit-Value of one Customer	100
$NLV_i(r)$	Net-rebate-Loss-Value of one Customer	10
K^{RS}	Cost per Customer for Rebate Strategy	2

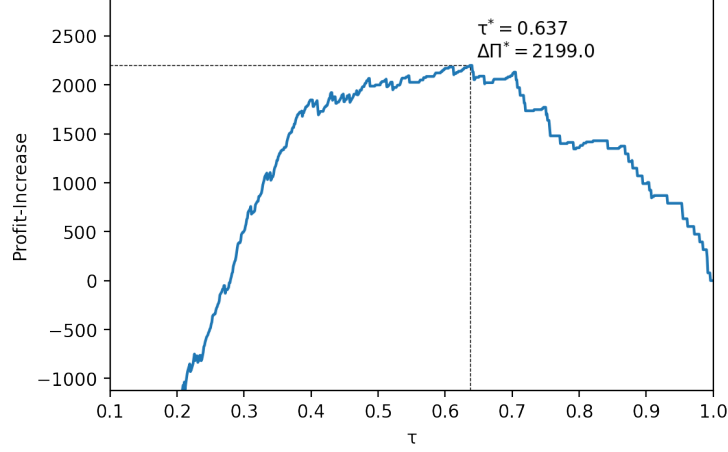
Table 10: Parameters for Profit-Increase-Simulation

The profit-increase to the status-quo due to the model deployment is therefore:

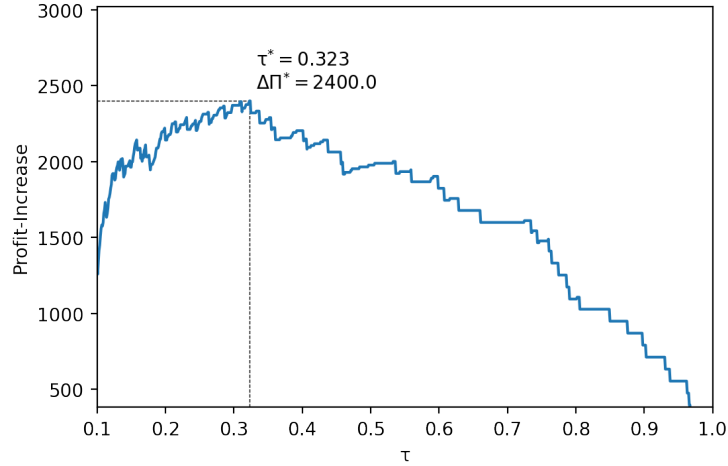
$$\begin{aligned}
\Delta\Pi(r, \tau) &= \sum_{i=1}^{N^{\hat{C}=1}} p^{prec} p_i^{succ} (NPV_i - NLV_i) - (1 - p^{prec}) NLV_i - K^{RS} \\
&= N^{\hat{C}=1} (91 p^{prec} - 12)
\end{aligned} \tag{18}$$

A modeler should search for the τ which maximizes equation (18). It lies in

the nature of almost all classification models, that $N^{\hat{C}=1}(\tau)$ negatively depends on τ and $p^{prec}(\tau)$ has a positive relationship with τ . We again plot the profit increase for 1000 candidates between 0 and 1 for both GBT's and EBM's candidate in figure 16.



(a) GBT



(b) EBM

Figure 16: Profit Increase in Simulation for different τ 's

For our simplified simulation the EBM candidate ensures the highest profit increase with a cutoff value $\tau = 0.323$. There, with the unseen data at hand, 39% of churners are detected, and the model predicts with a precision of 45%. Of course, when this simulation approach is applied in practice, the parameters in table 10 should be estimated correctly first. This could result in GBT reaching the profit maximizing cutoff and other optimal precision and recall metrics. The simulation is just an example on how to assess which model has

the better KPI-performance and for which cutoff this is ensured.

5 Conclusion

This work presents an applied machine learning approach on a well-studied customer churn prediction problem. The emphasize besides high predictive performance is on the predictive power of quotation data on the one hand and interpretability of the modelling approach on the other hand.

For the data set and the problem at hand we give insights on all approaches and steps used to get to the reached results. This includes the data preparation, modelling structure, sampling methods, dimension reduction, cost-sensitive loss-functions, machine learning models, evaluation metrics and interpretability approaches. After following the modelling structure, we present two candidate models, one for GBT and one for EBM. Both best candidates are achieved with sampling methods and a simple log loss as the objective.

In this work we show that quotation data has high predictive power. We therefore want to stress the importance of including it in any form of explanatory variables. We highly recommend companies and institutions to set up data warehouses which capture quotation activity of customers, which can be used to reflect the current behavior of them. To ensure that the predictive power is generalizable for all companies we want to motivate data collection and further research. The goal is to design a benchmark study on multiple independent data sets examining the benefit of quotation data.

We also show that for our application, EBM is able to outperform GBT in the OOS F1-Score. Eventhough it is not able to capture higher order interactions like GBT, EBM also reaches a higher profit-increase in our simplified simulation. For this application, the use of EBM dominates GBT because it additionally is more interpretable. Reliable interpretability opens up the opportunity to detect the main drivers leading to churn and to have a higher set of possible strategies to reduce it.

Furthermore, we want to declare one possible extension of this work which contains a different modelling approach. The idea is to model the events giving the customer the right of mid-contract termination separately. In the tree diagram of figure 17 we show how the event sequence leading to a churn is

constructed.

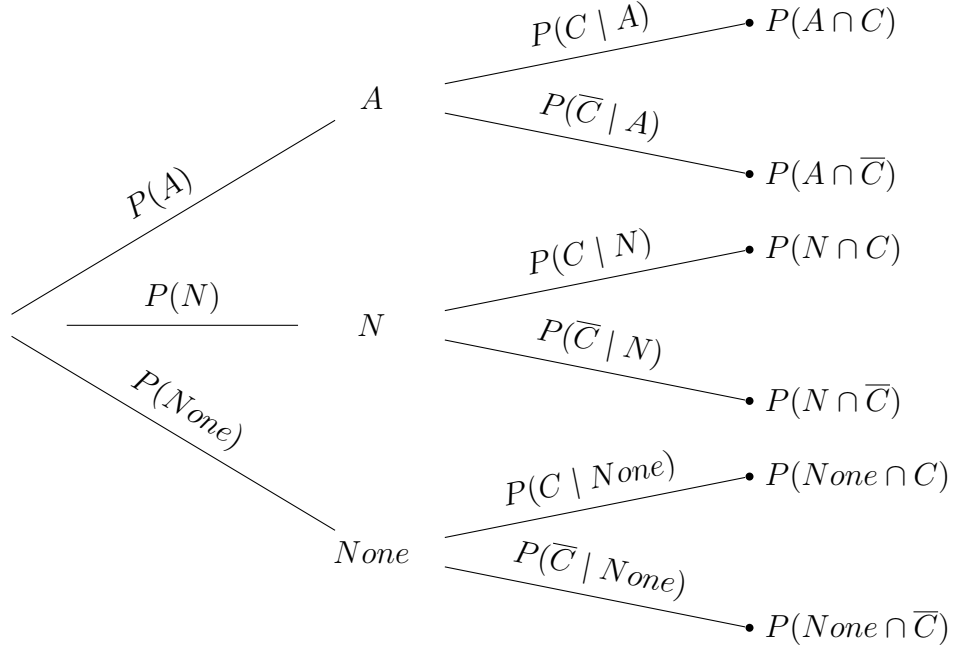


Figure 17: Tree Diagram of Events in the mid-contract Churn Setting

The tree diagram illustrates how the probability of a churn before the due date can be decomposed using the Events A (Accident), N (New Car) and C (Churn). By assumption we set $P(C | None) = 0$ as the amount of terminated contracts during the year which are not being caused by a new car, an accident or a due date is very small and can be omitted. What we are interested in predicting is the overall probability of a churn, which can be rewritten as:

$$\begin{aligned}
 P(C) &= P(C \cap A) + P(C \cap N) \\
 &= P(A)P(C | A) + P(N)P(C | N)
 \end{aligned} \tag{19}$$

The extension is to separately model $P(A)$, $P(C | A)$, $P(N)$ and $P(C | N)$. The best modelling approaches for an accident ($P(A)$) and for a new car ($P(N)$) in $(t, t + s]$ might differ in terms of models, sets of explanatory variables, sampling methods etc. Not only the unconditional but also the conditional probabilities $P(C \cap A)$ and $P(C \cap N)$ may vary in their best modelling approach. Predicting these 4 probabilities separately can also generate more interpretable insights to the main drivers for a churn. The probability of a

churn can be easily recomputed using these 4 quantities and equation (19).

References

- [1] Kendrick Boyd, Kevin H Eng, and C David Page. “Area under the precision-recall curve: point estimates and confidence intervals”. In: *Joint European conference on machine learning and knowledge discovery in databases*. Springer. 2013, pp. 451–466.
- [2] Leo Breiman. “Random forests”. In: *Machine learning* 45.1 (2001), pp. 5–32.
- [3] Jonathan Burez and Dirk Van den Poel. “Handling class imbalance in customer churn prediction”. In: *Expert Systems with Applications* 36.3 (2009), pp. 4626–4636.
- [4] Laura Calzada-Infante, Maria Oskarsdottir, and Bart Baesens. “Evaluation of customer behavior with temporal centrality metrics for churn prediction of prepaid contracts”. In: *Expert Systems with Applications* 160 (2020), p. 113553.
- [5] Nitesh V Chawla et al. “SMOTE: synthetic minority over-sampling technique”. In: *Journal of Artificial Intelligence Research* 16 (2002), pp. 321–357.
- [6] Kristof Coussement, Stefan Lessmann, and Geert Verstraeten. “A comparative analysis of data preparation algorithms for customer churn prediction: A case study in the telecommunication industry”. In: *Decision Support Systems* 95 (2017), pp. 27–36.
- [7] Aaron Fisher, Cynthia Rudin, and Francesca Dominici. “All Models are Wrong, but Many are Useful: Learning a Variable’s Importance by Studying an Entire Class of Prediction Models Simultaneously.” In: *Journal of Machine Learning Research* 20.177 (2019), pp. 1–81.
- [8] Jerome H Friedman. “Greedy function approximation: a gradient boosting machine”. In: *Annals of Statistics* (2001), pp. 1189–1232.
- [9] Jerome H Friedman and Bogdan E Popescu. “Predictive learning via rule ensembles”. In: *The Annals of Applied Statistics* 2.3 (2008), pp. 916–954.
- [10] Theresa Gattermann-Itschert and Ulrich W. Thonemann. “How training on multiple time slices improves performance in churn prediction”. In: *European Journal of Operational Research* 295.2 (2021), pp. 664–674.
- [11] Trevor J Hastie. *Generalized additive models*. Routledge, 2017.

- [12] Giles Hooker. “Generalized functional anova diagnostics for high-dimensional functions of dependent variables”. In: *Journal of Computational and Graphical Statistics* 16.3 (2007), pp. 709–732.
- [13] ZHOU Jie et al. “Customer churn prediction model based on lstm and cnn in music streaming”. In: *DEStech Transactions on Engineering and Technology Research* aemce (2019).
- [14] Harry Khamis. “Measures of Association: How to Choose?” In: *Journal of Diagnostic Medical Sonography* 24.3 (2008), pp. 155–162.
- [15] Samira Khodabandehlou and Mahmoud Zivari Rahman. “Comparison of supervised machine learning techniques for customer churn prediction based on analysis of customer behavior”. In: *Journal of Systems and Information Technology* (2017).
- [16] Tsung-Yi Lin et al. “Focal loss for dense object detection”. In: *Proceedings of the IEEE international conference on Computer Vision*. 2017, pp. 2980–2988.
- [17] Wei-Yin Loh. “Regression trees with unbiased variable selection and interaction detection”. In: *Statistica sinica* (2002), pp. 361–386.
- [18] Yin Lou et al. “Accurate intelligible models with pairwise interactions”. In: *Proceedings of the 19th ACM SIGKDD international conference on Knowledge discovery and data mining*. 2013, pp. 623–631.
- [19] Scott M Lundberg and Su-In Lee. “A unified approach to interpreting model predictions”. In: *Proceedings of the 31st International Conference on Neural Information Processing Systems*. 2017, pp. 4768–4777.
- [20] Helder Martins. “Predicting user churn on streaming services using recurrent neural networks”. In: (2017).
- [21] C Gary Mena et al. “Churn prediction with sequential data and deep neural networks. a comparative analysis”. In: (2019).
- [22] Christoph Molnar. *Interpretable machine learning*. Lulu. com, 2020.
- [23] Scott A Neslin et al. “Defection detection: Measuring and understanding the predictive accuracy of customer churn models”. In: *Journal of Marketing Research* 43.2 (2006), pp. 204–211.
- [24] Harsha Nori et al. “InterpretML: A Unified Framework for Machine Learning Interpretability”. In: (Sept. 2019).

- [25] Marco Tulio Ribeiro, Sameer Singh, and Carlos Guestrin. "Why should i trust you?" Explaining the predictions of any classifier". In: *Proceedings of the 22nd ACM SIGKDD International Conference on Knowledge Discovery and Data Mining*. 2016, pp. 1135–1144.
- [26] Cynthia Rudin. "Stop explaining black box machine learning models for high stakes decisions and use interpretable models instead". In: *Nature Machine Intelligence* 1.5 (2019), pp. 206–215.
- [27] Lloyd S Shapley. *17. A value for n-person games*. Princeton University Press, 2016.
- [28] Daria Sorokina et al. "Detecting statistical interactions with additive groves of trees". In: *Proceedings of the 25th international conference on Machine learning*. 2008, pp. 1000–1007.
- [29] Fei Tan et al. "A blended deep learning approach for predicting user intended actions". In: *2018 IEEE international conference on data mining (ICDM)*. IEEE. 2018, pp. 487–496.
- [30] Nguyen Thai-Nghe, Zeno Gantner, and Lars Schmidt-Thieme. "Cost-sensitive learning methods for imbalanced data". In: *The 2010 International joint conference on Neural Networks (IJCNN)*. IEEE. 2010, pp. 1–8.
- [31] Dirk Van den Poel and Bart Lariviere. "Customer attrition analysis for financial services using proportional hazard models". In: *European journal of Operational Research* 157.1 (2004), pp. 196–217.
- [32] Wouter Verbeke et al. "Building comprehensible customer churn prediction models with advanced rule induction techniques". In: *Expert systems with applications* 38.3 (2011), pp. 2354–2364.
- [33] veronica s moertini veronica s and niko ibrahim niko. "efficient techniques for predicting suppliers churn tendency in e-commerce based on website access data". In: *Journal of Theoretical & Applied Information Technology* 74.3 (2015).
- [34] HaiYing Wang. "Logistic Regression for Massive Data with Rare Events". In: *International Conference on Machine Learning*. PMLR. 2020, pp. 9829–9836.
- [35] Artit Wangperawong et al. "Churn analysis using deep convolutional neural networks and autoencoders". In: (2016).

- [36] Gary M Weiss. “Mining with rarity: a unifying framework”. In: *ACM Sigkdd Explorations Newsletter* 6.1 (2004), pp. 7–19.
- [37] Jacob Zahavi and Nissan Levin. “Applying neural computing to target marketing”. In: *Journal of direct marketing* 11.1 (1997), pp. 5–22.
- [38] Jaime Zaratiegui, Ana Montoro, and Federico Castanedo. “Performing highly accurate predictions through convolutional networks for actual telecommunication challenges”. In: (2015).
- [39] Yongbin Zhang et al. “Behavior-based telecommunication churn prediction with neural network approach”. In: *2011 International Symposium on Computer Science and Society*. IEEE. 2011, pp. 307–310.
- [40] Zhenyu Zhao, Radhika Anand, and Mallory Wang. “Maximum relevance and minimum redundancy feature selection methods for a marketing machine learning platform”. In: *2019 IEEE International Conference on Data Science and Advanced Analytics (DSAA)*. IEEE. 2019, pp. 442–452.
- [41] Bing Zhu, Bart Baesens, Aimée Backiel, et al. “Benchmarking sampling techniques for imbalance learning in churn prediction”. In: *Journal of the Operational Research Society* (2017), pp. 1–17.

Appendix

A. Gradient and Hessian for Weighted Loss Function

Simple Weighted Loss Function for one sample:

$$l(C, \hat{C}) = -(\alpha C \log(\hat{C}) + (1 - \alpha)(1 - C) \log(1 - \hat{C}))$$

We perform a few transformations to simplify the derivation:

$$\alpha_j = \begin{cases} \alpha, & C = 1 \\ 1 - \alpha, & C = 0 \end{cases}, \quad \hat{C}_j = \begin{cases} \hat{C}, & C = 1 \\ 1 - \hat{C}, & C = 0 \end{cases}$$

This way the loss simplifies to:

$$l(C, \hat{C}) = -\alpha_j \log(\hat{C}_j)$$

Again, consider following rewriting and note these functional relationships:

- $\hat{C}_j = \frac{\hat{C}(C+1)}{2} + \frac{(1-\hat{C})(1-C)}{2}$
- $\hat{C} = \frac{1}{1+e^{-g(X)}}$

The Gradient $\frac{\partial l}{\partial g(X)}$ then can be calculated with the chain rule with:

- $\frac{\partial l}{\partial \hat{C}_j} = -\frac{\alpha_j}{\hat{C}_j}$
- $\frac{\partial \hat{C}_j}{\partial \hat{C}} = \frac{C+1}{2} + \frac{C-1}{2} = C$
- $\frac{\partial \hat{C}}{\partial g(X)} = \frac{1}{1+e^{-g(X)}} \left(\frac{1+e^{-g(X)}}{1+e^{-g(X)}} - \frac{1}{1+e^{-g(X)}} \right) = \hat{C}(1 - \hat{C}) = \hat{C}_j(1 - \hat{C}_j)$

$$\boxed{\frac{\partial l}{\partial g(X)} = \frac{\partial l}{\partial \hat{C}_j} \cdot \frac{\partial \hat{C}_j}{\partial \hat{C}} \cdot \frac{\partial \hat{C}}{\partial g(X)} = -\frac{\alpha_j}{\hat{C}_j} \cdot C \cdot \hat{C}_j(1 - \hat{C}_j) = -\alpha_j C(1 - \hat{C}_j)}$$

The Hessian $\frac{\partial^2 l}{\partial g(X)^2}$ is calculated as:

$$\boxed{\frac{\partial^2 l}{\partial g(X)^2} = \frac{\partial}{\partial \hat{C}_j} \left(\frac{\partial l}{\partial g(X)} \right) \cdot \frac{\partial \hat{C}_j}{\partial \hat{C}} \cdot \frac{\partial \hat{C}}{\partial g(X)} = \alpha_j C^2 \hat{C}_j(1 - \hat{C}_j)}$$

Appendix

B. Gradient and Hessian for Focal Loss Function

Focal Loss Function for one sample:

$$l(C, \hat{C}) = - \left(\alpha(1 - \hat{C})^\gamma C \log(\hat{C}) + (1 - \alpha)\hat{C}^\gamma(1 - C) \log(1 - \hat{C}) \right)$$

We perform the same transformations to simplify the derivation:

$$\alpha_j = \begin{cases} \alpha, & C = 1 \\ 1 - \alpha, & C = 0 \end{cases}, \quad \hat{C}_j = \begin{cases} \hat{C}, & C = 1 \\ 1 - \hat{C}, & C = 0 \end{cases}$$

This way the loss simplifies to:

$$l(C, \hat{C}) = -\alpha_j(1 - \hat{C})^\gamma \log(\hat{C}_j)$$

Consider following rewriting and note these functional relationships:

- $\hat{C}_j = \frac{\hat{C}(C+1)}{2} + \frac{(1-\hat{C})(1-C)}{2}$
- $\hat{C} = \frac{1}{1+e^{-g(X)}}$

The Gradient $\frac{\partial l}{\partial g(X)}$ then can be calculated with the chain rule with:

- $\frac{\partial l}{\partial \hat{C}_j} = \alpha_j(1 - \hat{C}_j)^\gamma \left(\frac{\hat{C}_j \log(\hat{C}_j)^\gamma + \hat{C}_j - 1}{\hat{C}_j(1 - \hat{C}_j)} \right)$
- $\frac{\partial \hat{C}_j}{\partial \hat{C}} = \frac{C+1}{2} + \frac{C-1}{2} = C$
- $\frac{\partial \hat{C}}{\partial g(X)} = \frac{1}{1+e^{-g(X)}} \left(\frac{1+e^{-g(X)}}{1+e^{-g(X)}} - \frac{1}{1+e^{-g(X)}} \right) = \hat{C}(1 - \hat{C}) = \hat{C}_j(1 - \hat{C}_j)$

$$\boxed{\frac{\partial l}{\partial g(X)} = \frac{\partial l}{\partial \hat{C}_j} \cdot \frac{\partial \hat{C}_j}{\partial \hat{C}} \cdot \frac{\partial \hat{C}}{\partial g(X)} = -\alpha_j(1 - \hat{C}_j)^\gamma \left(\hat{C}_j \log(\hat{C}_j)^\gamma + \hat{C}_j - 1 \right) C}$$

The Hessian $\frac{\partial^2 l}{\partial g(X)^2}$ is calculated as:

$$\boxed{\begin{aligned} \frac{\partial^2 l}{\partial g(X)^2} &= \frac{\partial}{\partial \hat{C}_j} \left(\frac{\partial l}{\partial g(X)} \right) \cdot \frac{\partial \hat{C}_j}{\partial \hat{C}} \cdot \frac{\partial \hat{C}}{\partial g(X)} = \\ & \left(\alpha_j C \gamma (1 - \hat{C}_j)^{\gamma-1} \left(\gamma \hat{C}_j \log(\hat{C}_j) + \hat{C}_j - 1 \right) \right) C \hat{C}_j (1 - \hat{C}_j) + \\ & \left(\alpha_j C (1 - \hat{C}_j)^\gamma \left(\gamma \log(\hat{C}_j) + \gamma + 1 \right) \right) C \hat{C}_j (1 - \hat{C}_j) \end{aligned}}$$

Appendix

C. GBT Perfomance Improvement with Quotation Data

Model	Test-Set	Accuracy	Precision	Recall	F1	AUROC	AUPRC
gbt_u10_aNgN	OOS	0.53%	194.56%	184.62%	189.86%	6.53%	351.17%
	OOP	0.60%	162.24%	84.62%	117.94%	4.05%	236.61%
gbt_d0.1_aNgN	OOS	0.08%	85.24%	145.00%	105.23%	3.72%	270.13%
	OOP	0.32%	117.86%	131.25%	122.96%	1.77%	241.30%
gbt_u_aNgN	OOS	4.16%	59.73%	13.79%	54.85%	7.56%	416.18%
	OOP	5.39%	69.30%	12.07%	62.63%	5.32%	226.48%
gbt_d0.1_a0.6gN	OOS	-1.97%	$\infty\%$	$\infty\%$	$\infty\%$	80.65%	3140.41%
	OOP	-2.41%	$\infty\%$	$\infty\%$	$\infty\%$	71.53%	1544.56%
gbt_u_a0.8gN	OOS	55.41%	141.81%	-18.28%	131.91%	4.06%	450.51%
	OOP	54.86%	99.01%	-29.81%	90.49%	1.41%	331.83%
gbt_u50_aNg0.5	OOS	0%	0%	0%	0%	0.15%	0.92%
	OOP	0%	0%	0%	0%	-0.50%	-2.34%
gbt_sm_aNg2	OOS	3.86%	30.67%	12.33%	29.67%	4.06%	112.34%
	OOP	3.34%	8.76%	-5.00%	7.95%	2.13%	57.36%
gbt_u50_a0.6g1	OOS	20.43%	58.90%	-37.67%	50.04%	5.97%	37.30%
	OOP	21.37%	39.93%	-43.53%	31.95%	6.83%	25.93%
gbt_sm_a0.7g2	OOS	0%	0%	0%	0%	0%	0%
	OOP	0%	0%	0%	0%	0%	0%

Table 11: GBT-Candidates Improvement with Quotation Data

Appendix

D. EBM Performance Improvement with Quotation Data

Model	Test-Set	Accuracy	Precision	Recall	F1	AUROC	AUPRC
ebm_none	OOS	0.15%	$\infty\%$	$\infty\%$	$\infty\%$	19.37%	1488.73%
	OOP	0.08%	-23.53%	1200.00%	1044.78%	10.13%	373.36%
ebm_d0.1	OOS	0.03%	54.59%	109.52%	75.78%	18.54%	176.50%
	OOP	0.31%	97.12%	100.00%	98.43%	12.29%	174.12%
ebm_d0.5	OOS	0.14%	$\infty\%$	$\infty\%$	$\infty\%$	26.08%	1691.67%
	OOP	0.02%	5.88%	1700.00%	1318.54%	14.26%	475.47%
ebm_d	OOS	5.30%	21.48%	1.22%	20.50%	3.24%	20.97%
	OOP	6.01%	18.75%	-2.20	17.65%	1.88%	15.41%
ebm_u10	OOS	0.35%	92.26%	100.00%	95.35%	16.56%	209.98%
	OOP	0.64%	124.63%	75.00%	101.49%	9.60%	158.12%

Table 12: EBM-Candidates Improvement with Quotation Data